DESIGN AND CFD ANALYSIS OF BIMETALLIC BASED PASSIVE DYNAMIC COLD PLATE FOR HIGH POWER DIRECT-TO-CHIP LIQUID COOLING

by

APURV PRAVIN DESHMUKH

Presented to the Faculty of the Graduate School of

The University of Texas at Arlington in Partial Fulfillment

Of the Requirements

For the Degree of

MASTER OF SCIENCE IN MECHANICAL ENGINEERING

THE UNIVERSITY OF TEXAS AT ARLINGTON

AUG 2021

Supervising Committee:

Dr. Dereje Agonafer
Dr. Abdolhossein Haji-Sheikh
Dr. Miguel Amaya

Copyright © by APURV PRAVIN DESHMUKH, 2021

All Rights Reserved

Acknowledgments

Aug 16, 2021

I would like to Thank Dr. Dereje Agonafer for his support and supervision he provided me throughout the time of my research in EMNSPC Lab. I would also like to thank him for helping me with my thesis report and providing valuable tips for improving my work. I am particularly thankful towards him for introducing me with various prospects to learn and recognize the practices used in the electronic cooling field.

I would like to thank Dr. A. Miguel and Dr. A. Haji Sheikh for providing me with their valuable guidance in improving my work.

I would like to thank Mr. Pardeep Shahi, Mr. Satyam Saini and Mr. Pratik Bansode for being my mentors and guiding me all over my time at EMNSPC Lab and assisting me to put up this report.

Lastly, I would like to thank my parents Mr. Pravin Deshmukh and Mrs. Anita Deshmukh and my brother Amey Deshmukh for believing in me and supporting me in every part of my life.

Abstract

DESIGN AND CFD ANALYSIS OF BIMETALLIC BASED PASSIVE DYNAMIC COLD PLATE FOR HIGH POWER DIRECT-TO-CHIP LIQUID COOLING

(Reprinted with permission © 2021 ASME) [42]

APURV PRAVIN DESHMUKH

The University of Texas at Arlington, 2021

Supervising Professor: Dereje Agonafer

Rising demand for high-performance chips results in the need for advanced and efficient cooling technologies like direct to chip liquid cooling. Cold plates based utilizing direct liquid cooling is one of the most efficient and the most investigated cooling technology since the 1980s. Major data services and cloud providers like IBM, Microsoft, and Google had already started a shift towards liquid-cooled data centers for their high computational servers. At the chip level nowadays, the processors are divided into several cores and each of these cores continuously works at varying computational demands. This creates a non-uniform heat distribution across the processor, thus, developing a temperature gradient on and around the processor. This can lead to localized thermal transients and even thermo-mechanical failures in the worst cases to cyclic thermal stresses. This situation arises because the present-day cold plates provide the same flow rate irrespective of the IT load which is usually redundant and causes excessive water and energy usage. Therefore, to achieve uniform temperature distribution and achieve optimal cooling flow rates, new techniques are needed, and this can be done by the

deployment of dynamic cold plates. In this paper a concept of self-regulatory flow control strategy using bimetal strips is introduced. The proposed novel cold plate design and the damper will dynamically change the coolant flow rate to each section according to temperature in that section temperature. This design will not only reduce the thermal gradient on the processor but will also be beneficial in terms of equipment reliability.

List of Illustrations

Figure 1. Typical air cooled data center... 3

Figure 2. Liquid cooled data center 4

Figure 3. Schematic of placement of cold plate... 5

Figure 4. CoolIT cold Plate.. 5

Figure 5. IR thermal camera image of actual CPU (left) and Thermal profile of Die (right)…………………………………………………………………………………….....7

Figure 6. ANSYS OptiSlang design points... 9

Figure 7. Nitinol Spring with Damper configuration for dynamic flow control 11

Figure 8. Proposed nitinol spring and damper working principle 12

Figure 9. Working principle of bimetal 14

Figure 10. Bimetal 3D model... 20

Figure 11. Material properties of GB alloy in ANSYS workbench.................................... 19

Figure 12. Material properties of 14 alloy in ANSYS workbench 19

Figure 13. Thermal loading on bimetal model... 20

Figure 14. Constrain on the geomtry 21

Figure 15. Result of the bimetal simulation for directional deformation in Z-axis 22

Figure 16. Temperature Vs Deflection plot for different lengths of bimetal 22

Figure 17. Modified cold plate for V-shape bimetal configuration..23

Figure 18. ANSYS Icepack simulation setup...24

Figure 19. ANSYS Icepack simulation setup-Source... 25

Figure 20. Meshing of the fins.. 26

Figure 21. Geometry used in no bimetal condition simulation.. 29

Figure 22 Temperature plot at the base of the cold plate in no-bimetal condition simulation 29

Figure 23. Revised design of the cold plate 30

Figure 24. Revised design cold plate simulation for no-bimetal condition. 31

Figure 25. Final assembly model of revised cold plate design 31

Figure 26. Dimensioning details of middle plate 32

Figure 27. Dimensioning details of middle plate 32

Figure 28. position of the blocks to replicate the opening created by bimetal........ 36

Figure 29. Top surface of middle plate CASE 1 @ 1 lpm........ 37

Figure 30 Top surface of middle plate CASE 2 @ 1 lpm........ 38

Figure 31. Top surface of middle plate CASE 3 @ 1 lpm........ 38

Figure 32. Top surface of middle plate CASE 4 @ 1 lpm........ 39

Figure 33. Top surface of middle plate CASE 5 @ 1 lpm........ 39

Figure 34 CASE 1 No bimetal (left), CASE 1 With bimetal (right) 40

Figure 35. CASE 1 No bimetal (left), CASE 2 With bimetal (right) 41

Figure 36. CASE 1 No bimetal (left), CASE 3 With bimetal (right)........ 41

Figure 37. CASE 1 No bimetal (left), CASE 4 With bimetal (right) 42

Figure 38 CASE 1 No bimetal (left), CASE 5 With bimetal (right) 42

Figure 39. ΔT *for all the cases at all lpm* 43

Figure 40. Rth for all the cases at all the lpm. 44

Figure 41. % Changes in temperature gradient for all the cases. 44

List of Tables

Table 1. List of the flow control strategies. 18

Table 2. List of the bimetal suggestion from EMS Inc 16

Table 3. Chemical composition of GB14 16

Table 4. Thermostatic properties of GB14 17

Table 5. Physical properties of GB14 17

Table 6. Mesh properties for bimetal simulation 20

Table 7. Mesh sensitivity analysis for bimetal simulation 21

Table 8. Different Cases for different load conditions 25

Table 9. Mesh properties for cold plate simulation 27

Table 10. No bimetal condition temperature results @0.6 lpm 33

Table 11. No bimetal condition temperature results @0.8 lpm 34

Table 12. No bimetal condition temperature results @1 lpm 34

Table 13. No bimetal condition temperature results @1.2 lpm 35

Table 14. No bimetal condition temperature results @1.5lpm 35

Table 15. GB14 deflection at specific temperatures 37

Table of Contents

Acknowledgments iii

Abstract iv

List of Illustrations vi

List of Tables ix

Chapter 1 Introduction 1

1.1 Air cooling for data center 2

1.2 Why Liquid cooling for high power data center? 3

Chapter 2 Objective of the study- Need of the dynamic liquid cooling 7

Chapter 3 Design of Dynamic Cold plate 8

3.1 Study of flow control strategies 10

3.1.1 Nitinol spring and damper configuration 11

3.1.2 Bimetallic strip configuration 14

3.2 Design of the cold plate for V-shape bimetal configuration 23

3.3 CFD Analysis of cold plat on Ansys Icepack 24

3.3.1 Results of the CFD analysis of the cold plate for no-bimetal condition 28

3.3.2 Simulation results for all the cases for No-bimetal condition 33

3.3.3 Simulation for with bimetal condition for all the cases 36

3.3.4 Comparison between No-bimetal and with-bimetal cases 40

Chapter 4 Conclusion and Future work 45

References 47

Chapter 1

Introduction

The use of the data centers has increased since the last decade. The rise in technology such as AI, 3D mapping, neural networking, machine learning, crypto mining has led the data processing even more complicated. This all such applications required tremendous amount of power and all the tech- giants has realized that the data processing and data storage in next human need. The importance of data has become extremely vital than ever before and to stand beside all processing need, the power density on the processing unit such as CPUs, GPUs are also increased significantly. Current trend in advancement are clearly indicates that this growth will continue to increase. Now a days, the highest operating temperature on the chip is allowed to exceed 100~120° C and due to increase in temperature across the module the reliability and the performance issue are two major concern all industry is facing.

The proposed dynamic cold pate design is a 3-part assembly that is divided into three main sections. The bottom section of the plate contains 4 different sections of parallel copper microchannels through which the coolant flows, extracting the heat. The novel cold plate design and the damper will dynamically change the coolant flow rate to each section according to temperature in that section, unlike traditional cold plates. This design will not only reduce the thermal gradient on the processor but will also be beneficial in terms of equipment reliability.

1.1 Air cooling for data center

The use of the data center has increased past few decades but almost 95% of the data center that currently operating are all air cooled. Air cooled data center construction is widely studied, and lot of research has been done on the that. Since air cooling has several other applications, people feel comfortable with air cooling for their application, and this also makes air cooling cost effective and reliable. Typical air cooling for any application contains several cooling units. In data center applications, server is stacked up in rack and several racks are placed together and this rack consumes huge amount of power. The typical air-cooled data center contains raised floor construction as shown in figure 1. Raised floor are made for air to pass thru it and allow rack to cool at different location. The computer room air conditioner (CRAC Unit) is present at each data center room which allows supply of cold air thru this raised floor. Data centers are divided into two aisle, cold aisle and hot aisle. As cold air enters raised floor it passes thru the cold aisle then heat is removed from the rack and passes to hot aisle. This hot air is then again collected by CRAC unit by natural convection and cooled down and cycle repeats. External chillers are used to perform necessary heat exchange in CRAC unit. Approximately 35 to 40 % energy that data center consumes consumed by the air-cooling technology that data center uses and due to increase in the demand of high-power data center this energy consume by the air cooling is also increasing. Processing units like CPUs, GPUs are consuming more power leading more heat generation and this effects the air-cooling limitation. Due to this the need of the new cooling technologies are currently taking lot of interest.

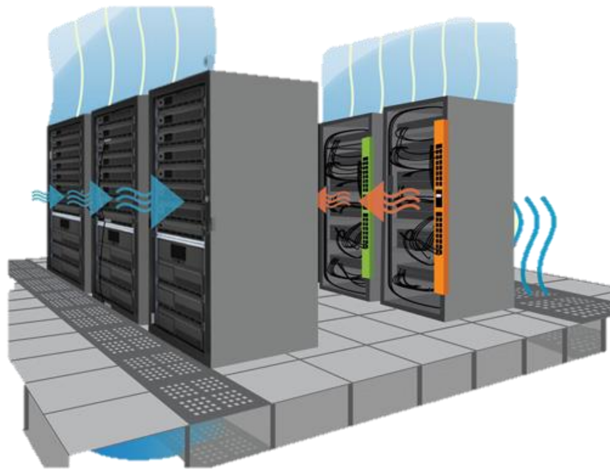

.

Figure 1 Typical air-cooled data center

1.2 Why Liquid cooling for high power data center?

Liquid cooling is already in use for many purposes and has proven effective solution for high power demand. Liquid cooling has many advantages over air cooling and since 1960 the technological advancement in CMOS and research in air cooling once again became a sustainable alternative [7-10]. The power on multi-module chip has increased and since Dennard's scaling is now fading, chip manufacturers are compensating their chip power to get improved performance with same chip area by increasing the number of transistors on the chip. This has significantly improved the use of the liquid cooling system in data center [11-13]. Apart from power density, liquid cooling would significantly improve the energy efficiency of the system because air cooling required substantial amount of power. As said earlier, due to increase in heat dissipation, chip performance and reliability are major two concerns arise in air cooling which may leads to thermal shutdown and system failure. Liquid cooling system also carries small number of units as compared to air cooling system therefore maintenance of the system also become much easier in

liquid cooling. The most significant difference between both liquid cooled and air-cooled data center is that it allows very reduced amount of noise level as compared to air cooling. Air cooled data center running at full capacity might reach the noise level up 85~90 dB which is harmful for human ear and work environment to be such high noise level is not desirable for any profession. Figure 2. Represents schematic of typical liquid cooled data center in which CDU (Coolant distribution unit) is used. It’s a liquid to liquid type heat exchanger which takes facility water roughly around 7-9 C and cools the coolant and passes thru the loop. The coolant first enters into Row manifold which distributes the coolant to each rack as shown in figure. Rack also has separate distribution system called as Rack manifold. Coolant enters to rack manifold thru row manifold via hoses and it has inlet and outlet port for each server. All these connections are typically made up of hoses and quick disconnect therefore handling and the assembly of these systems are fast and easy. Row manifold, Rack manifolds, CDU, all hose connections these are all external parts of the liquid cooling system but what responsible for the heat transfer inside the server is a cold plate. After entering the server, coolant again distributed to each cold plate thru cooling loop connection. Cold plate is usually micro-fin structure made up of copper, sometime aluminum. Coolant passes thru this fin, and heat transfer takes place and heated coolant is again supplied back to CDU thru rack and row manifolds as shown in figure 2. Figure 3. Represents the schematic of the cold plate mounting over the module and figure 4. Is the actual photo of the cold plate from company called CoolIT. The high specific heat of the liquid allows liquid cooling to be more efficient than air cooling and due to this large heat transfer is takes place in smaller area. Liquid cooled data center can be used as a hybrid data center in which high power module can be cooled using cold plate and for other components, air cooling with typical fan and heat sink arrangement could be implemented [14].

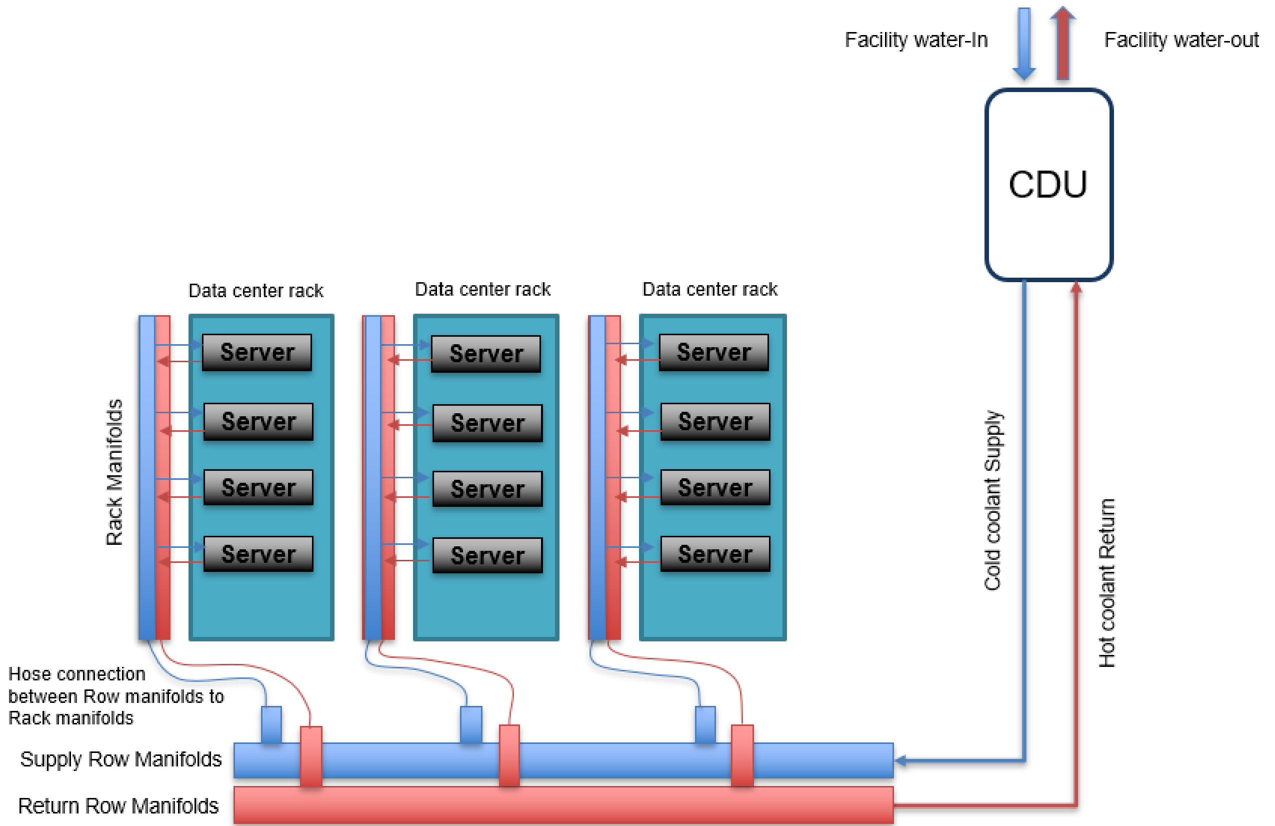

Figure 2. Liquid-cooled data center

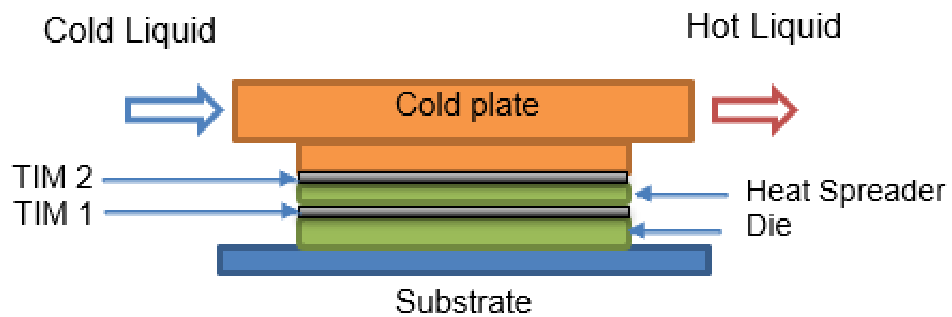

Figure 3. Schematic of placement of cold plate

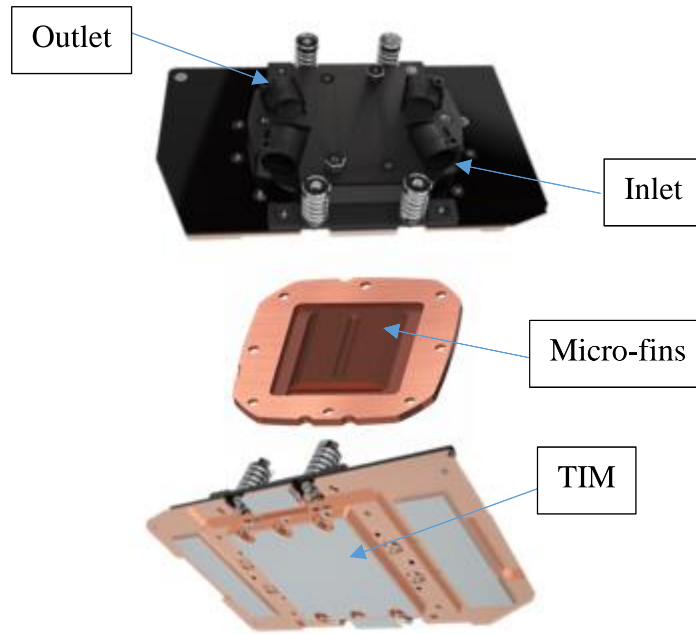

Figure 4. Image of cold Plate

Image source: CoolIT offical website.

Chapter 2

Objective of the study- Need of the dynamic liquid cooling

The most recent architecture advancement of new processing units contains multiple cores and different module on same chip. This advancement in microarchitectures enhanced the performance of the computing tremendously. But increase in number of different modules on single chip draws different power and creates multiple hotspots on the chip and due to such high temperature region, the performance, and the reliability of the chip, both becomes sever problem. To address this issue the study of the localize cooling at particular high temperature region in required. This such type of dynamic cooling was also executed in air cooling systems and 70% improvement in the performance of the data center was observed by controlling fan speed in air vents [15] Even after using liquid cooling as primary cooling system, we can still find the hot spot on the chip. Figure 5. Represent the thermal profile of the typical die where we can clearly see that the temperature across CPU module is much higher as compared to another module [16]. The research related dynamic cooling shows that the performance of such dynamic cooling system can be improved thru machine learning in which speed of the fan and related vent opening can be regulated [17-21]. Kasukurthy [22,23] in his paper studied similar dynamic cooling for liquid cooling and developed a control strategy and FCD which showed 64% of pumping power saving by controlling flow thru each server. In this study conceptual design of the dynamic flow control across the fins of the cold plate is proposed. Different types of the flow control strategies and temperature sensitive material are studied. The design of the fins in any cold plate are most crucial part of the study therefore design optimization study using ANSYS Opti-slang is performed, and fins are designed. This proposed dynamic cold plate not only improves the temperature gradient but also can reduce the thermal resistance of the cold plate significantly.

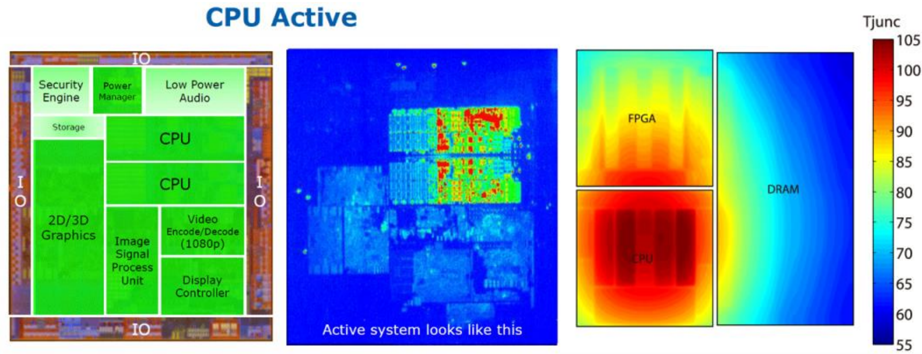

Figure 5.IR thermal camera image of actual CPU (left) and Thermal profile of Die (right) [15]

Chapter 3

Design of Dynamic Cold plate

The fins of the cold plate are most important part of the cold plate. All the necessary heat transfer is take place at micro channel fins thru which coolant passes. Therefore, design of the fins is crucial part in cold plate design. Design of the fins includes important parameter such as fin thickness, spacing between two fins, fin length. Apart from this, good cold plate also contains appropriate flow rate and pressure drop thru inlet and outlet. The dimension of the cold plate affects the pressure drop and pumping power. Therefore, proper optimization of the fin dimensions is necessary. Industry manufacturers usually uses 0.1 mm to 1 mm fin thickness but this calculation many times made up on experience bases. To get more robust and optimized model for this application, ANSYS OptiSlang design optimization is used. ANSYS OptiSlang is a very powerful tool and performs very time- consuming manual calculation and gives us best design configuration. Another beauty of this software is we can put many design constraints to get accurate results.

For this application following design variable are considered:

Fin thickness: 0.1 -1 mm

Fin Spacing: 0.2 – 1 mm

Inlet Velocity:0.029 – 1.91 m/s

Objective function was to minimize both, pressure drop and Max. temperature across cold plate.

Fig (1) show different design data point out of which optimum parameters are selected.

Fin Thickness: 0.48 mm

Fin Spacing: 0.48 mm

Inlet Velocity: 0.4 m/s

Inlet Pressure: 135.46 Pascal

Max. Temp.: 33.83 ℃

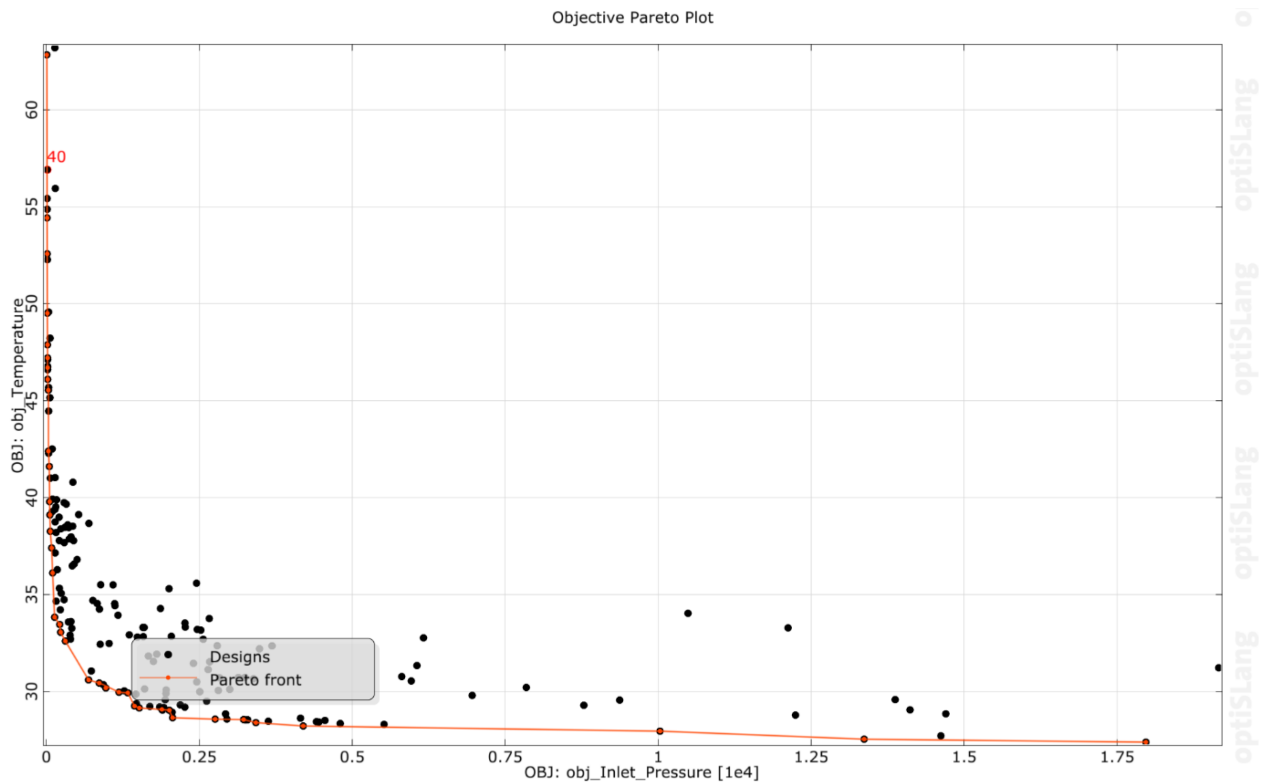

Figure 6. ANSYS OptiSlang design points

3.1 Study of flow control strategies

Wide number of flow control strategies for miniature flow control are available in industry. Out of which, some are listed below in the table 1. Most of the control strategies listed in the table requires external power to perform the necessary work. Although the actuation and deflection in electronic flow control strategies are much greater, energy required should also be considered. In this thesis the idea of the temperature sensing flow control is proposed using shape memory alloy and bimetallic strip. These are the only two type of flow control strategies that can be used without any external power input. Shape memory alloy remembers particular shape at particular temperature and bimetal deflects as temperature changes.

Actuation method	Stroke (Displacement)	Response time
Solenoid Plunger	Large	Fast
Disk type piezoelectric	Small	Fast
Pneumatic	Large	Slow
Shape Memory Alloy	Slow	Slow
Thermo-pneumatic	Medium	Medium
Electromagnetic	Large	Fast
Bimetallic Strip	Small	Medium

Table 1. List of the flow control strategies

After selecting shape memory alloy and bimetal to proceed with for dynamic flow control across the cold plate, multiple study on both the strategies are carried out to understand the material behavior and reliability of the flow control strategy. For dynamic flow control, accurate deflection at particular temperature is necessary otherwise we will find many differences in the flow at same temperature which eventually leads to unstable system.

3.1.1 Nitinol spring and damper configuration

Nitinol is a type of shape memory alloy which reacts to change in temperature and changes its shape. Nitinol changes its phase from martensite to austenite on temperature change. Nitinol also has two configurations, Two-way nitinol and One-way nitinol. Two-way nitinol remembers two different types of shape at low and high temperature whereas one-way nitinol remembers one specific shape at specific temperature. Nitinol spring is used in the previous study of the self-regulating FCD by Rushi [24] in 2018. To improve the proposed idea and modify the nitinol spring configuration in this dynamic cold plate design, a 3D model of the dynamic cold plate with nitinol spring and damper is proposed as shown in the figure 7.

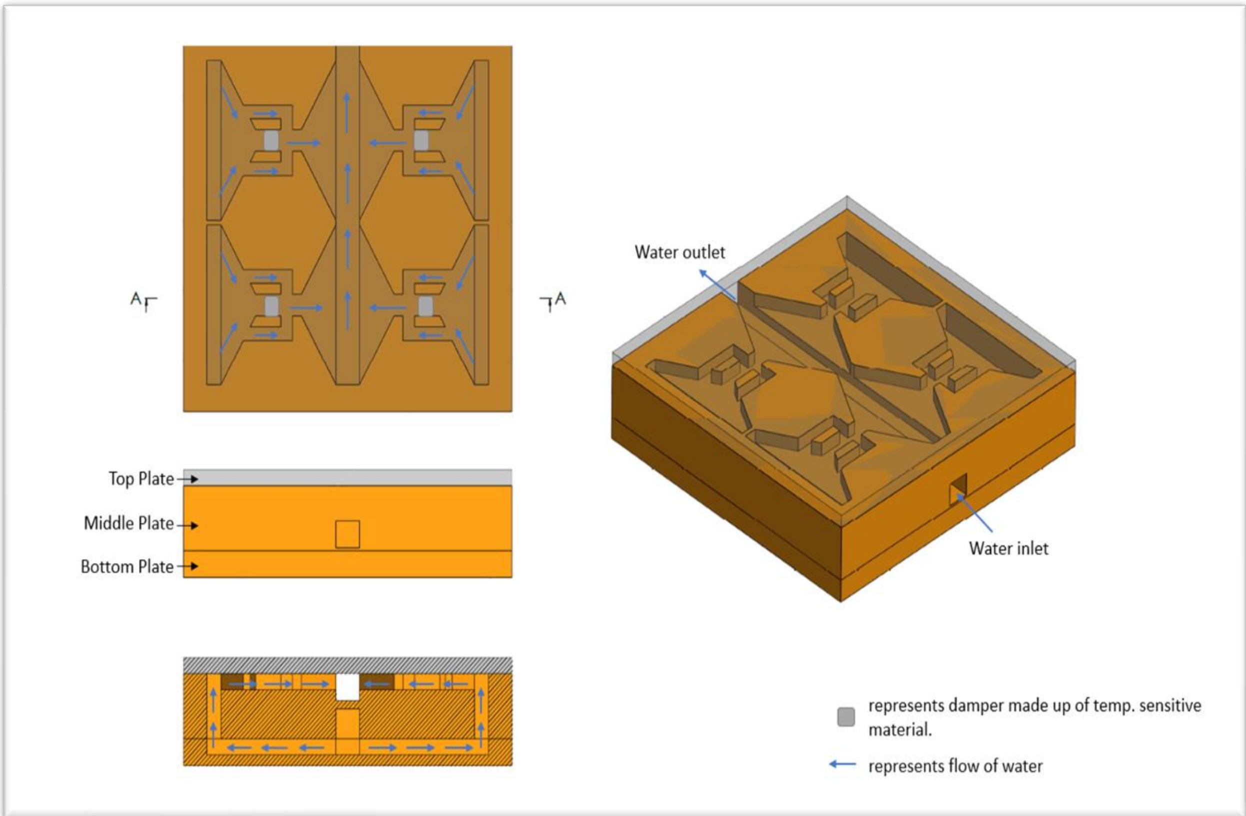

Figure 7. Nitinol Spring with Damper configuration for Dynamic flow control

As shown in figure 7, the design of the cold plate was modeled in 3 parts namely, bottom part, middle part and top part. The bottom part of the cold plate contains fins as per ANSYS OptiSlang results. Middle part is made in such a way that damper is will be connected to the nitinol spring and it will move to-and-fro to regulate the flow thru each 4 sections. Middle plate has inlet which allows flow to pass thru fins (bottom plate) and then rise up again to middle plate to each four-damper section. Thru damper section it will pass to common passage between four section which further leads to outlet. Figure 8. Represents scaled model of each section in middle plate and explains working principle of the proposed nitinol spring flow control model.

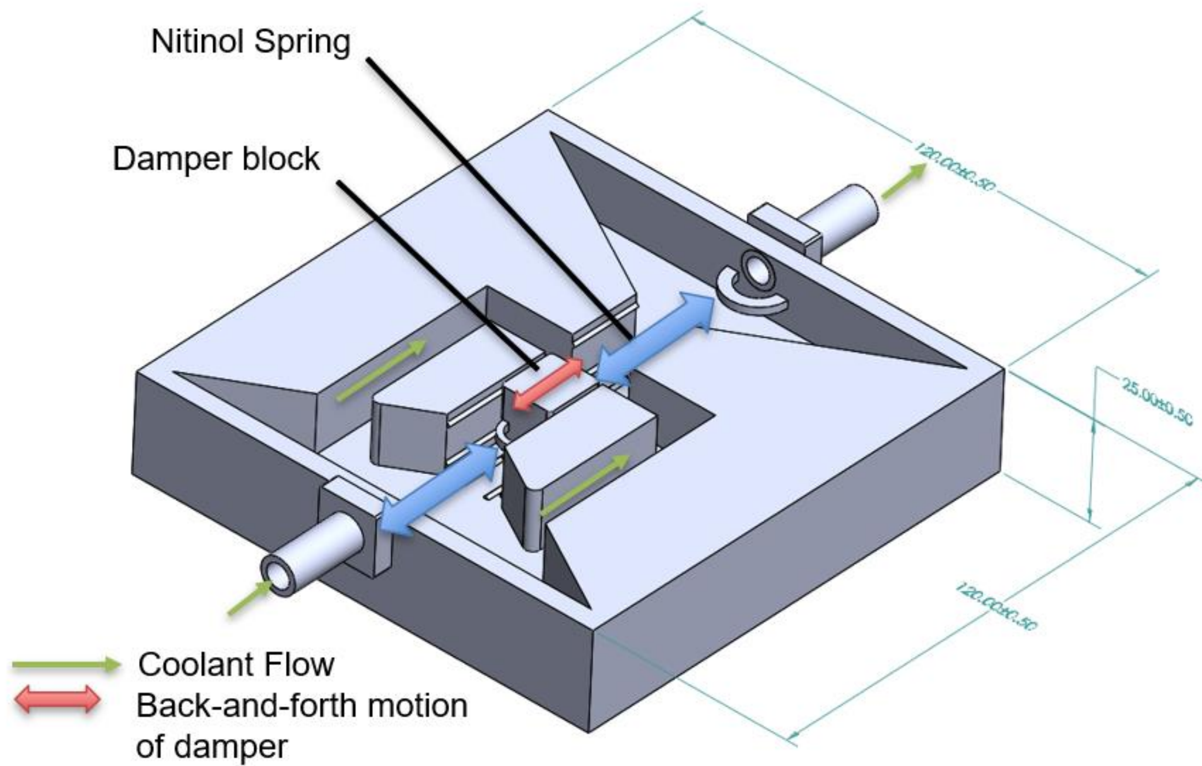

Figure 8. Proposed nitinol spring with damper working principle

The major issue that nitinol spring faced was the reliability. The experiment to predict the reliability of this model was found to be very difficult. Even the simulation of such nitinol spring is complicated to perform. The deflection of the nitinol spring with the respective temperature is found to be non-linear and the results of the study also unstable. To avoid such uncertainty and improve the reliability of the flow control strategy, Bimetallic strip configuration is proposed in further study.

3.1.2 Bimetallic strip configuration

The bimetal is the combination of the two different metals having two different CTE (coefficient of thermal expansion) values. Usually, the one metal has higher CTE value and the other has lower CTE value. This special feature of the bimetal allows it to deflect in different temperature conditions. Figure 9. Represents working principle of the bimetallic strip. The material are strongly bonded together and the material with lower CTE value restrict the motion of the higher CTE value as shown in figure. 9

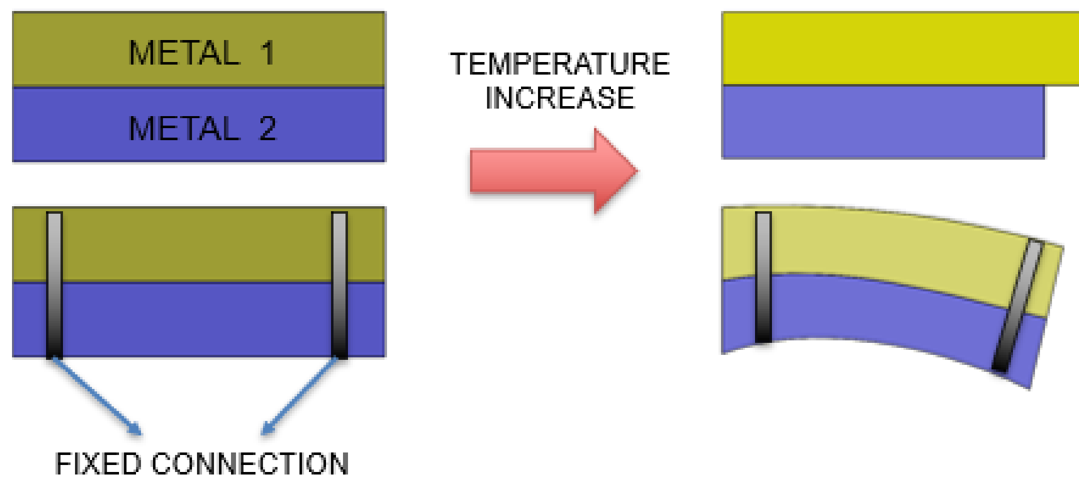

Figure 9. Working principle of bimetal

In above figure metal 1 has higher CTE value and material 2 has lower CTE value. Using bimetal, we can control flow thru very small region. Also, bimetal is widely use component and it has lot of industry applications. It does not require any external power to perform the deflection and it can be used as all-in-one device which could act as sensor, valve and actuator together. The construction of the bimetal is simple, and it is available in wide range of dimension and shape configurations, so reliability of the material is also not a big issue

3.1.2.1 Selection of the bimetal and shape configuration

Bimetals are also called as thermostat metal. While selecting the bimetal for applications few things are important. Tensile and compressive stresses in the bimetal are given by following formula:

$$\sigma = E/\,2\,(\alpha 1 - \alpha 2)\,(T2 - T1) \tag{1}$$

Flexivity which is a unique property of the bimetal defines the change in curvature of the longitudinal line of the material per unit temperature per unit thickness.

$$F = (1\,/R2 - 1\,/R1\,)\;\; t\,/(\;T2 - T1) \tag{2}$$

T1, T2 = initial and final temperature

t = total thickness

Formula for the radius is as follows,

$$1\,/\,R = 8D\,/\,(L^{2} + 4Dt + 4D^{2}) \tag{3}$$

D = deflection value at center

To decide accurate and compatible material with cold plate applications, external company support from bimetal manufacturer has been taken. Engineered material solution Inc. has guided the selection of the bimetal and as per their expertise suggestion GB14 alloy has finally selected. Table 2. Contains bimetal list provided by EMS Inc. Good deflection, i.e., good flexivity value and corrosion resistance in glycol-based solution are two main criteria was

set. GB14 is two-layer alloy bimetal in which alloy GB contain high CTE value and alloy 14 contain low CTE value.

Truflex Type	ASTM Flexivity F x 10^{-7} 50° - 200° F temp range	Maximum sensitivity temperature range °F	Useful deflection temperature range °F	Recommended maximum temp °F	Modulus of elast. E, lbs/sq.in by 10^6	Resistivity at 75°F ohms cm/ft.	Density lb./cu.in.	ASTM type	Remarks
F70R	147	0 to 300	-100 to 500	700	24.5	70	0.299	TM27	Low Electrical Resistivity and Medium Flexivity
F90R	148	0 to 300	-100 to 500	700	25.0	90	0.298	TM28	Low Electrical Resistivity and Medium Flexivity
F100R	149	0 to 300	-100 to 500	700	25.0	100	0.297	--	Intermediate Electrical Resistivity and Medium Flexivity
F125R	148	0 to 300	-100 to 500	700	25.0	125	0.297	--	Intermediate Electrical Resistivity and Medium Flexivity
F55R20	130	100 to 500	-100 to 700	700	22.0	54	0.300	--	Low Electrical Resistivity and Medium Flexivity
G7	61	0 to 800	-100 to 1000	1000	27.5	440	0.280	--	Linear flexivity 0-800°F
GB2	128	100 to 550	-100 to 1000	1000	26.0	445	0.295	--	General purpose 100° to 550°F (38° to 260°C). Good High Temperature Stability
GB5	75	300 to 800	-100 to 1000	1000	26.0	342	0.296	--	General purpose 300° to 800°F (150° to 425°C). Higher Flexivity than E5.
GB14	100	0 to 300	-100 to 1000	1000	26.0	511	0.294	--	Good corrosion resistance in aqueous environments
J1	134	0 to 300	-100 to 500	625	19.0	110	0.310	--	Low temperature only
J7	56	0 to 500	-100 to 500	625	22.0	106	0.300	--	Best corrosion resistance
LA1	158	0 to 300	-100 to 700	1000	25.0	475	0.292	TM29	Good all purpose 0-300°F

Table 2. List of the bimetal suggestion from EMS Inc.

Chemical Composition		
	Grade	**Chemistry**
High Expansion Alloy	Alloy GB	19% Ni, 7% Cr, Bal Fe
Low Expansion Alloy	Alloy 14	38% Ni, 7% Cr, Bal Fe

Table 3. Chemical composition of GB14

Table 3, 4 ,5 represent chemical, thermostatics, physical properties of the alloy. This data is provided by the company and later used in the simulation of the bimetal.

Thermostatic Properties		ENGLISH		METRIC	
ASTM Flexivity	(50-200°F)	100	x 10^{-7} (in/in)/°F	--	
	(100-300°F)	100	x 10^{-7} (in/in)/°F	--	
Specific Curvature	(10-93°C)	--		18.0	X 10^{-6} (mm/mm)/°C
	(38-149°C	--		18.0	X 10^{-6} (mm/mm)/°C
Maximum Sensitivity Temperature Range		0 to 300	°F	-20 to 150	°C
Useful Deflection Temperature Range		-100 to 1000	°F	-70 to 540	°C
Recommended Maximum Temperature		1000	°F	540	°C
Electrical Resistivity @ 75° (24°C)		486 to 536	OCMF*	0.808 to 0.891	μohms-m

.

Table 4. Thermostatic properties of GB14

Physical Properties	ENGLISH		METRIC	
Density	0.294	Lb/in^3	8.12	g/cm^3
Modulus of Elasticity (E)	26.0	Msi	179	GPa

Table 5. Physical properties of GB14

3.1.2.2 FEA analysis of the bimetal

After selecting the appropriate material, static structural analysis is carried out on V- shape bimetal. Figure 10 represents CAD model of the bimetal modeled using SolidWorks. The purpose of the FEA simulation was to predict the temperature vs deflection plot for different dimension of the bimetal. To perform this FEA simulation ANSYS Workbench was used. Material properties for GB14 alloy was taken from company data sheet and it is implemented in Ansys material list.

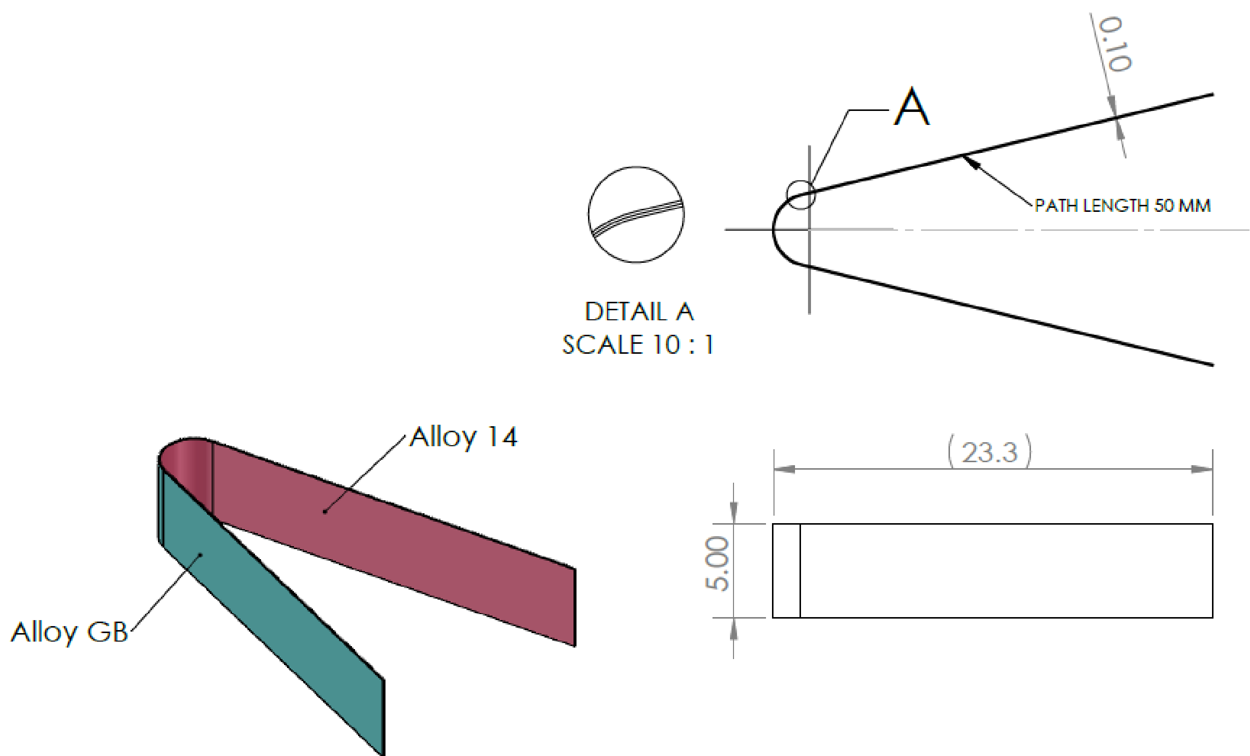

Figure 10. Bimetal 3D model

	A	B	C
1	Property	Value	Unit
2	Material Field Variables	Table	
3	Density	7.7	g cm^-3
4	Isotropic Secant Coefficient of Thermal Expansion		
5	Coefficient of Thermal Expansion	1.02E-05	F^-1
6	Isotropic Elasticity		
7	Derive from	Young's Modulus and Poisson's Ratio	
8	Young's Modulus	1.79E+11	Pa
9	Poisson's Ratio	0.3	
10	Bulk Modulus	1.4917E+11	Pa
11	Shear Modulus	6.8846E+10	Pa

Figure 11 Material Properties of the GB alloy in Ansys Workbench

	A	B	C
1	Property	Value	Unit
2	Material Field Variables	Table	
3	Density	7.7	g cm^-3
4	Isotropic Secant Coefficient of Thermal Expansion		
5	Coefficient of Thermal Expansion	3.5E-06	F^-1
6	Isotropic Elasticity		
7	Derive from	Young's Modulus and Poisson's Ratio	
8	Young's Modulus	1.79E+11	Pa
9	Poisson's Ratio	0.3	
10	Bulk Modulus	1.4917E+11	Pa
11	Shear Modulus	6.8846E+10	Pa

Figure 12. Material Properties of the 14 alloy in Ansys Workbench

Table 6. represents the meshing properties used for FEA simulation. Thermal loading is then applied as shown in figure 13. And the temperature range was set to 25 C to 70. For the fix support V shape end of the bimetal was fixed to give constrain to the simulation.

Mesh Properties	parameters
Mesh element size	0.08mm
No. of nodes	559920
Element Count	79002
Type of mesh	Rectangular

Table 6. Mesh properties for bimetal simulation

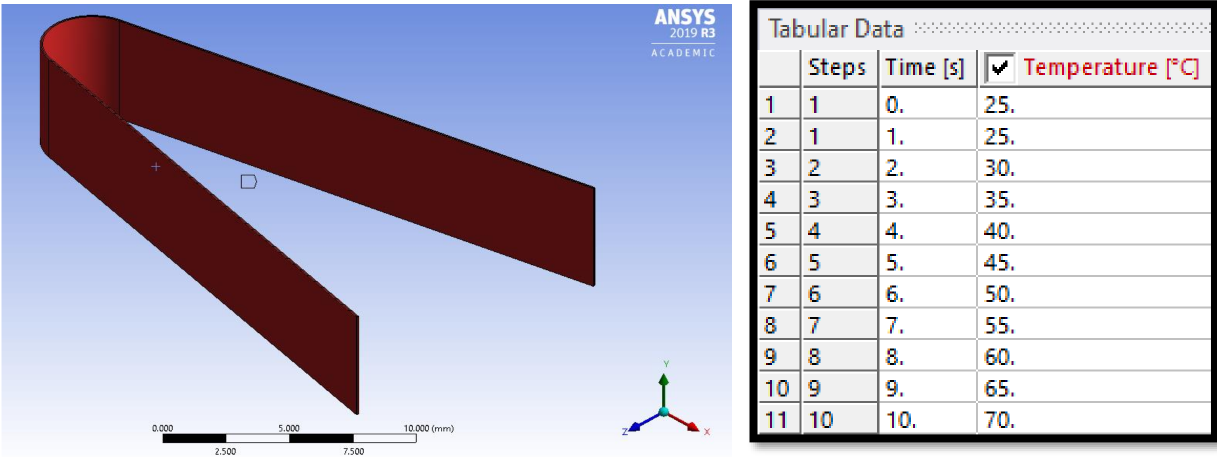

Tabular Data

	Steps	Time [s]	Temperature [°C]
1	1	0.	25.
2	1	1.	25.
3	2	2.	30.
4	3	3.	35.
5	4	4.	40.
6	5	5.	45.
7	6	6.	50.
8	7	7.	55.
9	8	8.	60.
10	9	9.	65.
11	10	10.	70.

Figure 13. Thermal loading on Bimetal model

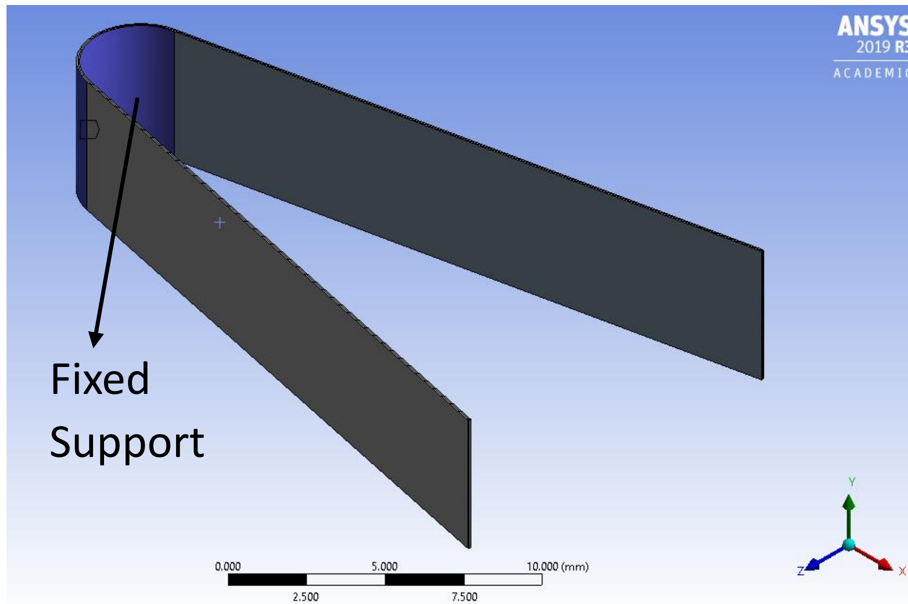

Figure 14. Constrains on the geometry

Mesh sensitivity study is performed on the model to confirm the number of the nodes and the number of the element are enough to get accurate results. Table 7. Represents the mesh sensitivity analysis.

Number of Elements	Max. Deflection. at 70 C
45236	2.054 mm
79002	2.2296 mm
120120	2.2297 mm
145638	2.2298 mm

Table 7. Mesh sensitivity analysis for bimetal simulation

3 simulations at 3 different length, 50 mm, 45 mm, and 40 mm were performed to compare the result of deflection at given temperature range. It is found that the increase in the length of the bimetal increase the deflection. Figure 16. Represents graph of the comparison between 3 bimetal configurations.

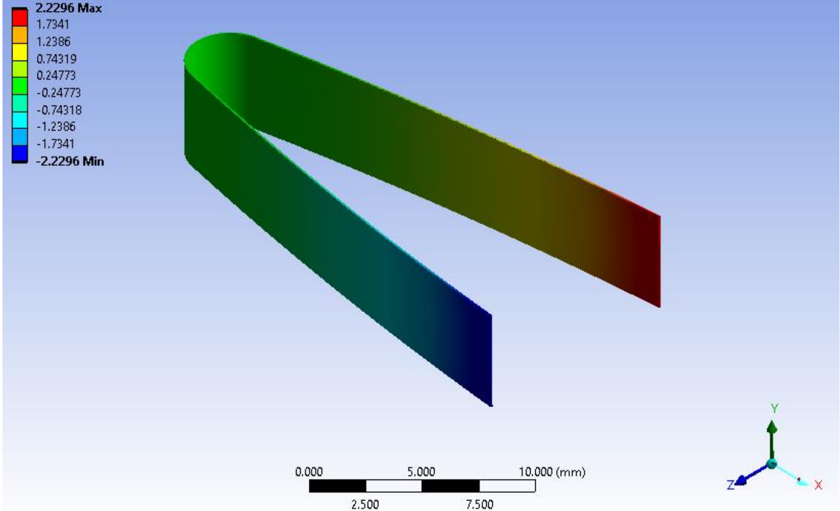

Figure 15. Result of the bimetal simulation for directional deformation in Z-axis

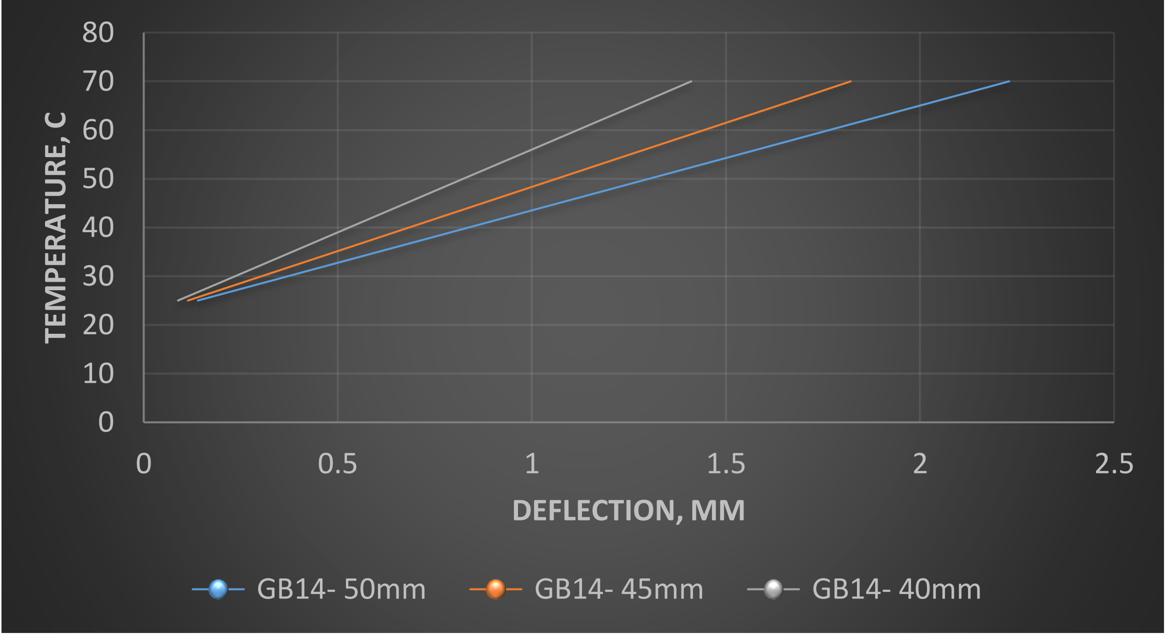

Figure 16. Temperature Vs Deflection plot for different lengths of bimetal

3.2 Design of the cold plate for V-shape bimetal configuration

The cold plate model was modified to accommodate V-shape bimetal. The bottom part of the design was kept similar and only middle plate was modified. The middle potion was change in such a way that the change in temperature at specific portion of the middle plate deflect the bimetal and regulates the flow of the coolant as required. Figure 17. Shows the 3D model of the modified model.

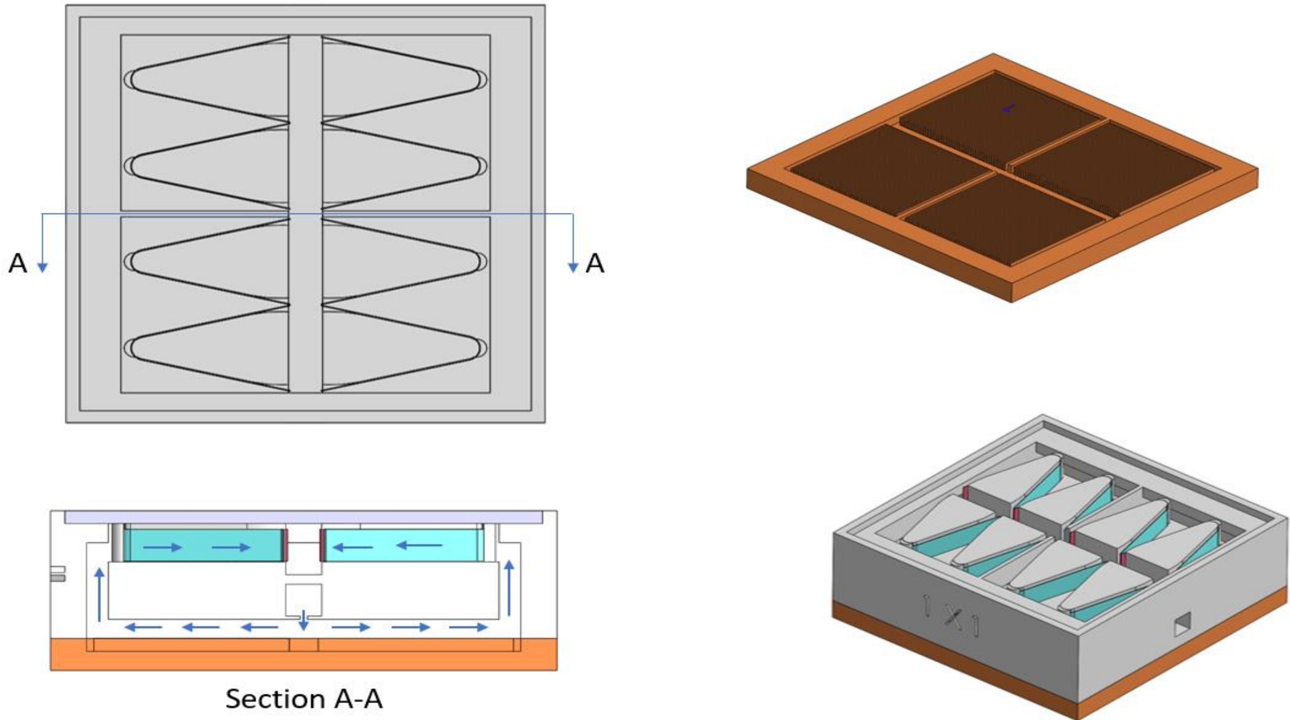

Figure 17. Modified cold plate for V-shape bimetal configuration

3.3 CFD Analysis of cold plat on Ansys Icepack

The simulation of the complete dynamic cold plate with the bimetal include found to be difficult because of it's dynamic nature. To simplify this process, first all the simulation without the bimetal was performed. The geometry from the solidworks is directly imported into ANSYS spaceclain and then it is simplified for Icepack simulation.

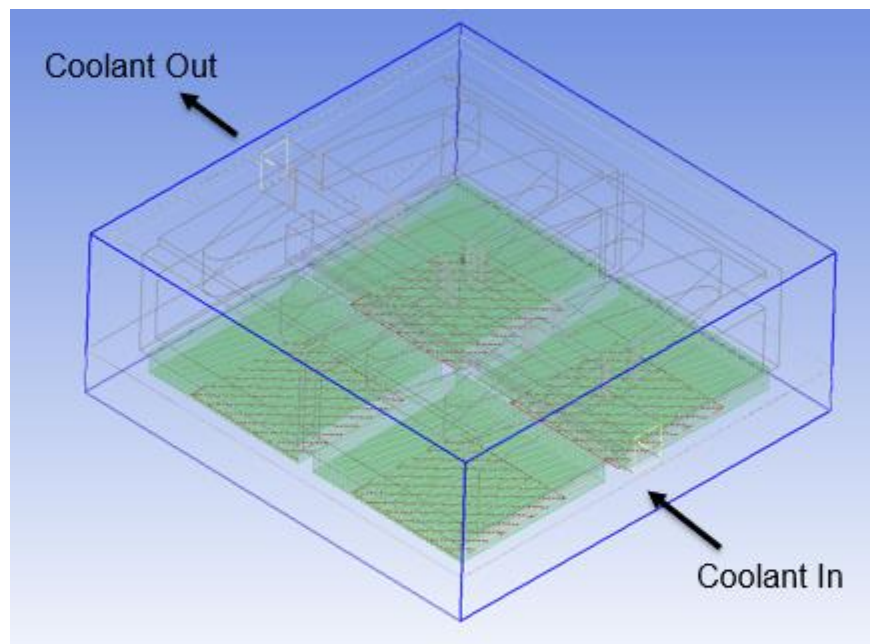

Figure 18. ANSYS Icepack simulation setup

4 Heat sources as shown in figure 19 was imported to perform different load condition. As we know multi-chip module creates lot of hot spots and to replicate that hot spot this heat sources are manual given different load conditions. Table 8 represents different load conditions used in the simulation.

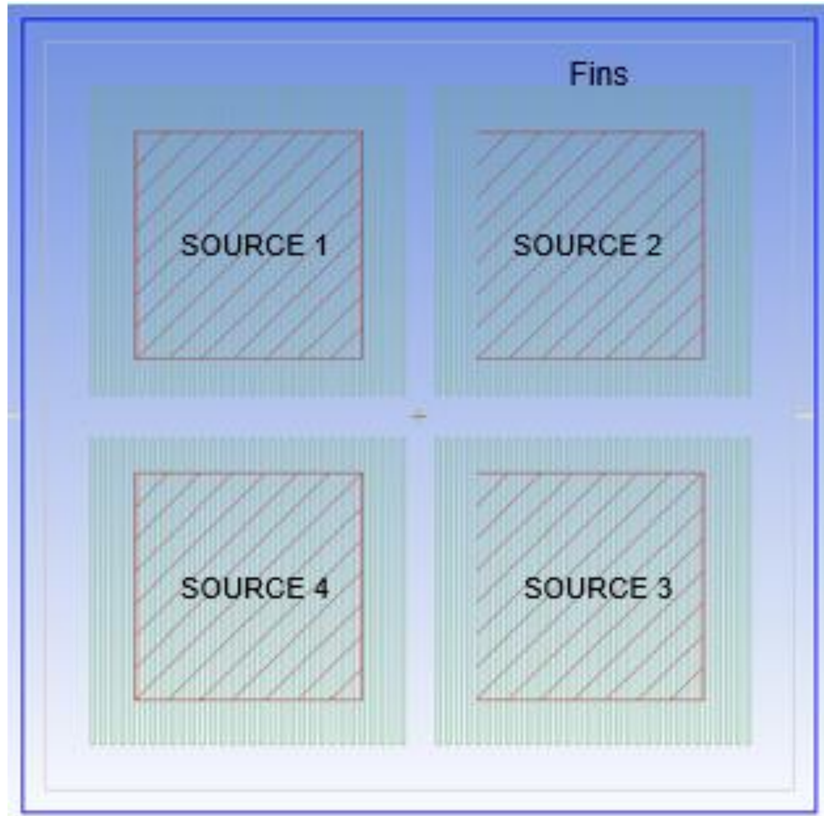

Figure 19. ANSYS Icepack simulation setup-Source

	Source 1	Source 2	Source 3	Source 4
Case 1	90 W	90 W	90 W	90 W
Case 2	10 W	10 W	90 W	90 W
Case 3	90 W	90 W	10 W	10 W
Case 4	10 W	90 W	10 W	90 W
Case 5	90 W	10 W	90 W	10 W

Table 8. Different Cases for different load conditions

For the meshing of the geometry, meshing around the fins was most critical part. To get accurate result around the fins, parametric pre-object meshing was applied on the fins and manual number of elements are given in each direction as shown in figure 20.

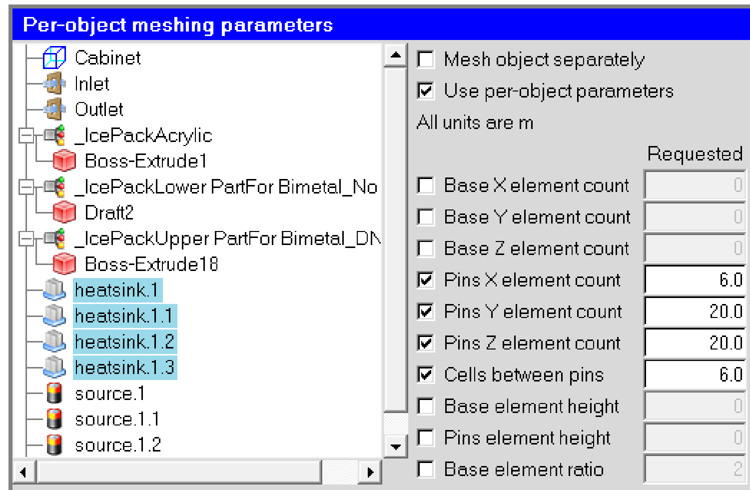

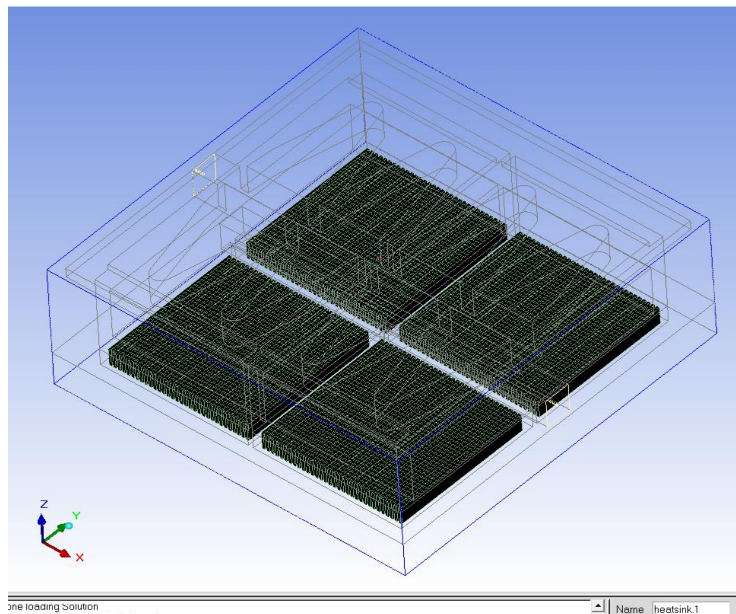

Figure 20. Meshing of the fins

Apart from fins table 9 represents other mesh properties used in the simulation.

Mesh Properties	parameters
Min. Mesh element size	0.04mm
No. of nodes	1634181
Element Count	1585020
Type of mesh	Rectangular

Table 9. Mesh properties for cold plate simulation

To perform no bimetal condition simulations, following boundary conditions and assumptions are made.

- Intel Velocity: 0.4 m/s
- Outlet Condition: Outflow
- Gravity Effect: ON
- Default Fluid: Water
- Flow Regime: Laminar
- Ambient Temperature: 25 C
- Water Inlet Temp: 25 C

- Material: Base Fins Plate – Cu, Middle plate- Bakelite, Upper Plate – Bakelite
- Heat transferred due to radiation are ignored
- Solution is solved for Steady-state condition
- Number of Iterations: 1500
- Convergence Criteria was set on 10E-6

3.3.1 Results of the CFD analysis of the cold plate for no-bimetal condition

It was observed that the temperature gradient across the cold plate was found to be very high.

Source 1 Max Temp. - 36.33 ^{o}C

Source 2 Max Temp. – 44.32 ^{o}C

Source 3 Max Temp. - 59.08 ^{o}C

Source 4 Max Temp. - 52.15 ^{o}C

$\Delta T = 59.08 - 36.33 = 22.75$ ^{o}C

ΔT was found to *22.75* ^{o}C which is pretty high for load condition shown in the figure 22.

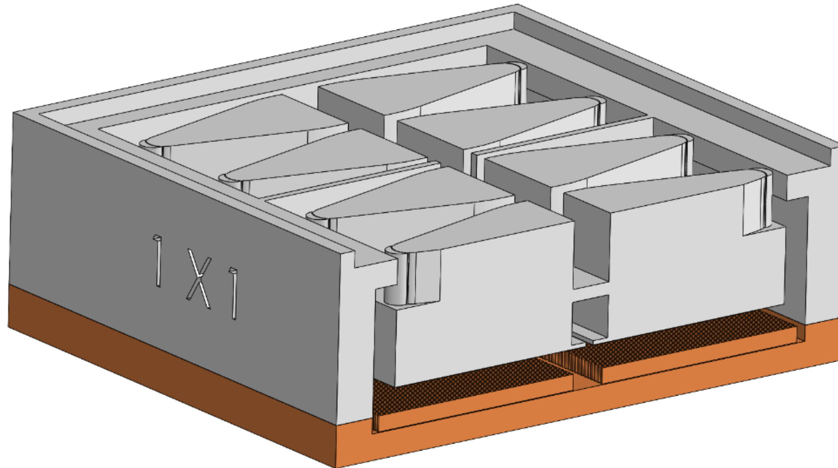

Figure 21. Geometry used in no bimetal condition simulation

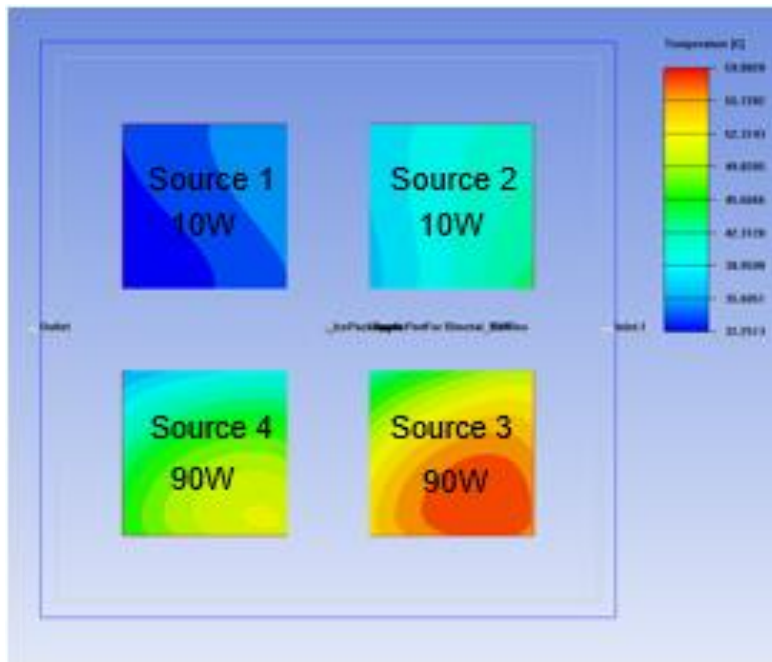

Figure 22. Temperature plot at the base of the cold plate in no-bimetal condition simulation

The possible reason to get this high temperature gradient was flow of the liquid found to be passes over the fins instead of going thru the fins. So the model of the cold plate was revised and the gap between the middle plate and the bottom plate was reduce.

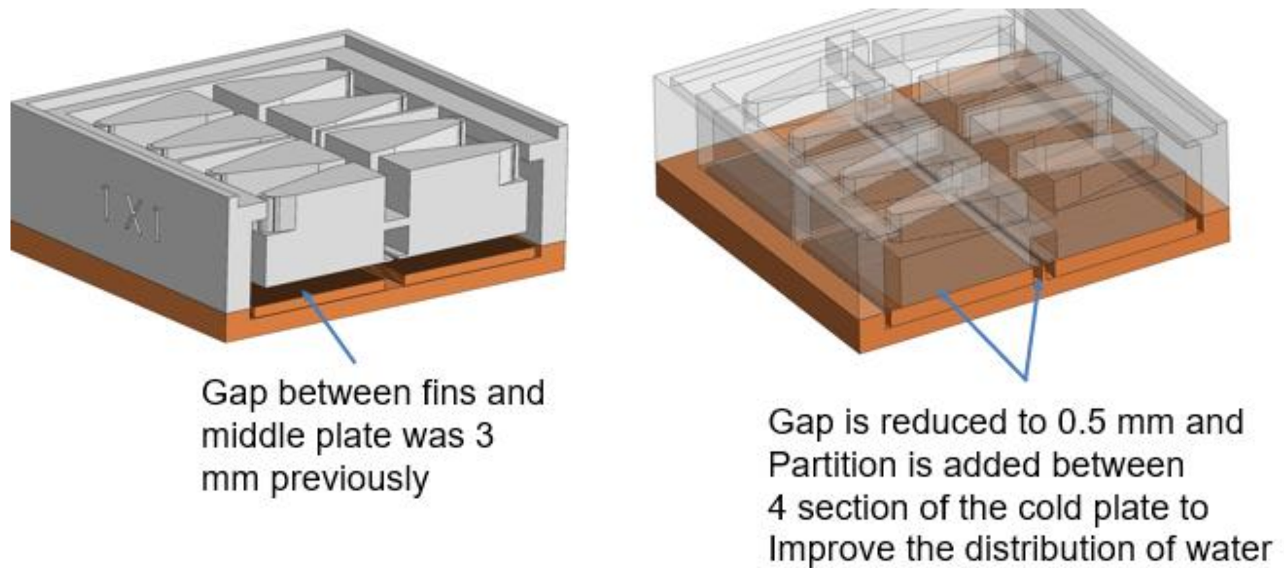

Figure 23. Revised design of the cold plate

Similar simulations to the previous simulation are performed again using this revised model and significant decrease in the temperature gradient was found.

Source 1 Max Temp. - 29.25 ºC

Source 2 Max Temp. – 33.98 ºC

Source 3 Max Temp. - 44.42 ºC

Source 4 Max Temp. - 38.35 ºC

$\Delta T = 44.42\text{-}29.25 = 15.17$ ºC

ΔT was reduced to *15.17* ºC from *22.75* ºC which is significant improvement. Figure 24 represents temperature plot for revised cold plate for similar load conditions as previous.

This cold plate design is later used for all the simulation. Figure 25 represents final assembly of the revised design.

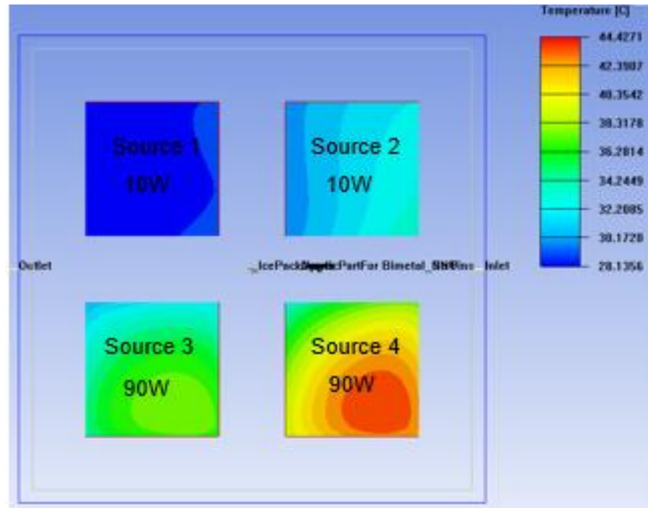

Figure 24. Revised design cold plate simulation for no-bimetal condition

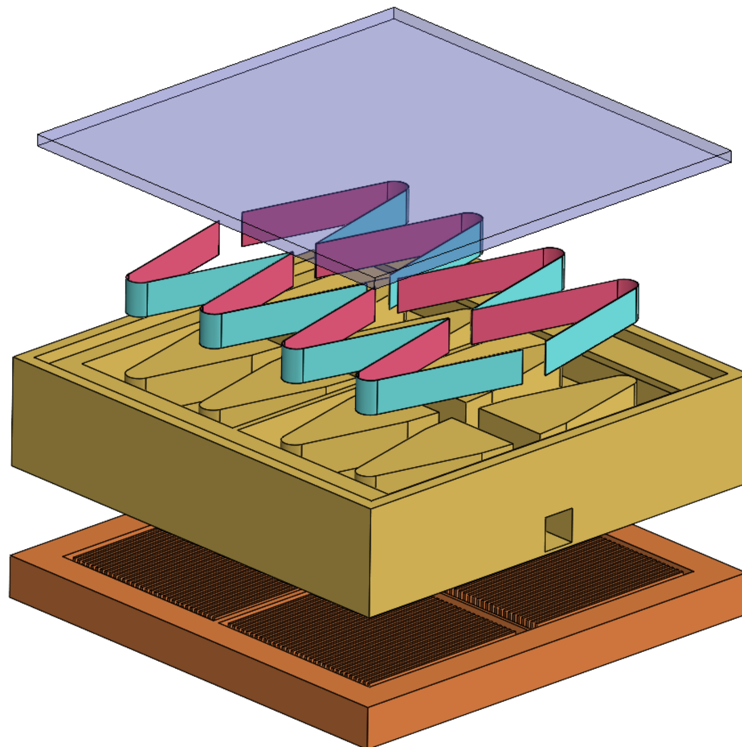

Figure 25. Final assembly model of revised cold plate design

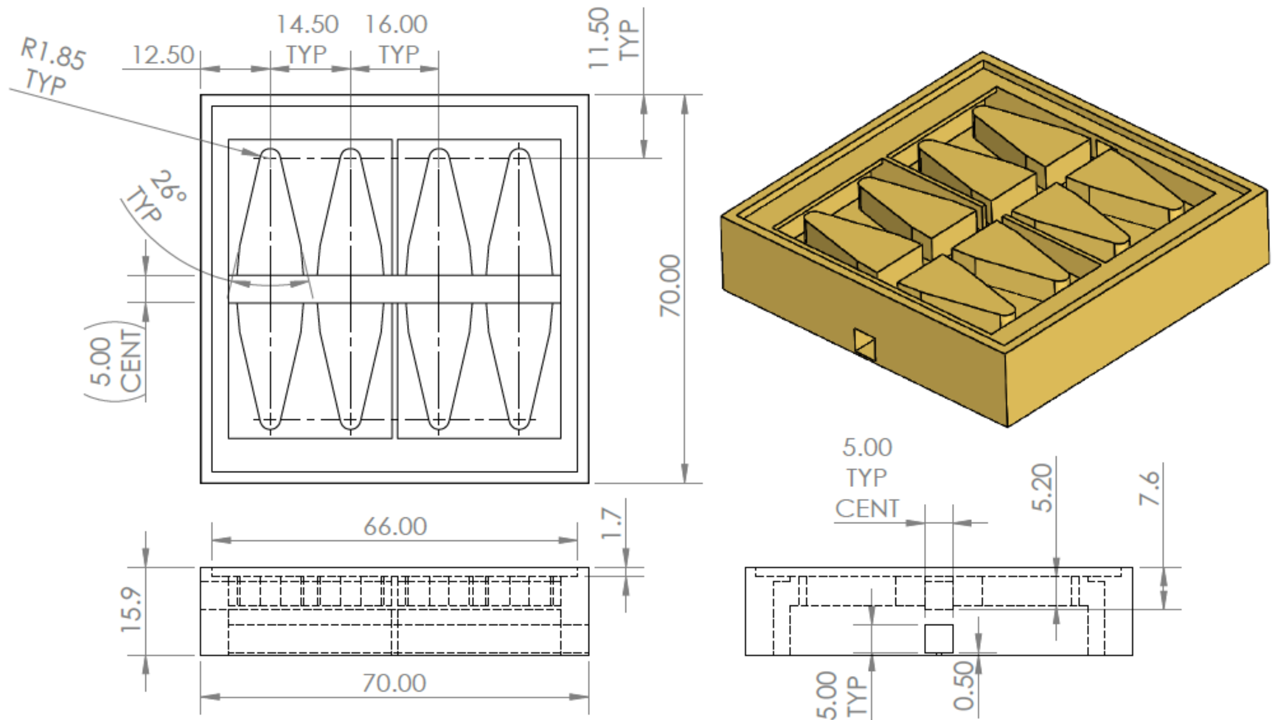

Figure 26. Dimensioning details of middle plate

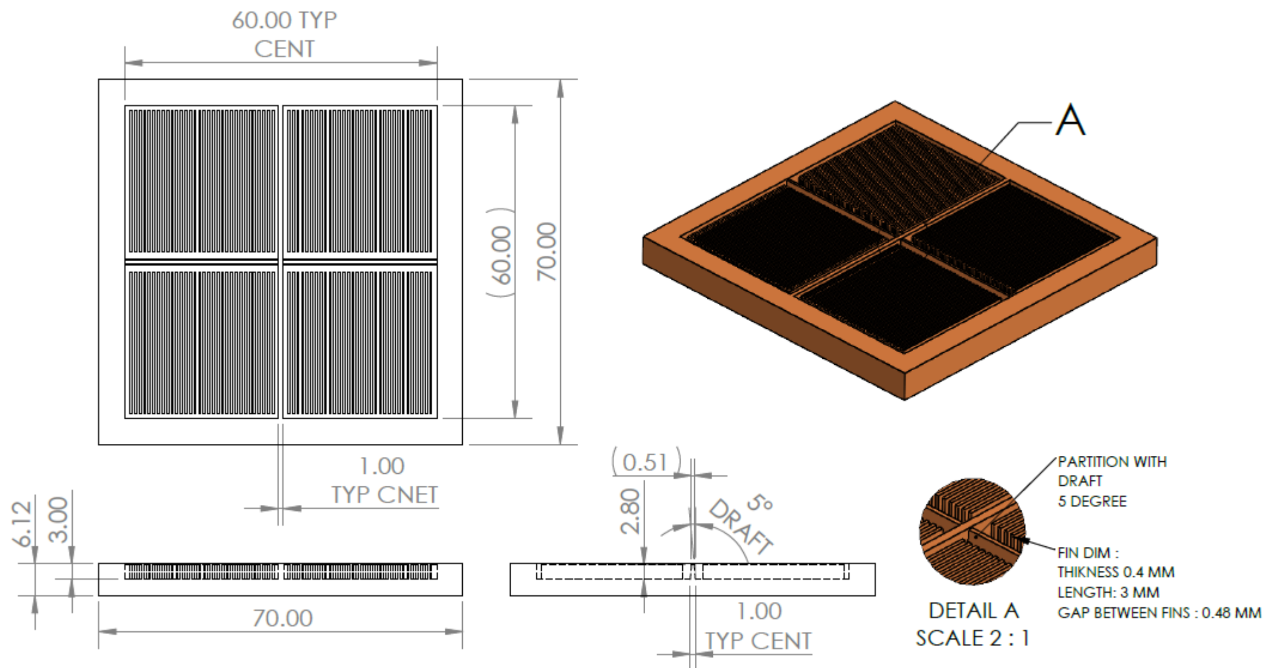

Figure 27. Dimensioning details of bottom plate

3.3.2 Simulation results for all the cases for No-bimetal condition

Five different cases at five are considered as shown in the table 7 to compare the results. This all five case simulated for 5 different flow rate, 0.6 lpm, 0.8 lpm, 1 lpm, 1.2 lpm, 1.5 lpm respectively.

No Bimetal_ 0.6 lpm					Delta T
	Source 1	Source 2	Source 3	Source 4	
Case 1	41.756	50.553	49.08	40.44	10.113
Case 2	29.255	33.983	44.4271	38.3561	15.1721
Case 3	39.7033	46.0669	34.3026	29.4201	16.6468
Case 4	32.5231	44.8412	34.3616	37.1981	12.3181
Case 5	38.145	34.3729	43.6492	31.7396	11.9096

Table 10. No bimetal condition temperature results @0.6 lpm

No Bimetal_ 0.8 lpm					Delta T
	Source 1	Source 2	Source 3	Source 4	
Case 1	39.3369	49.2547	47.3849	38.0786	11.1761
Case 2	28.4777	33.4314	43.191	36.5471	14.7133
Case 3	37.7959	45.1284	33.7156	28.618	16.5104
Case 4	31.4163	44.1043	33.7513	35.6074	12.688
Case 5	36.4487	33.7718	42.585	30.564	12.021

Table 11. No bimetal condition temperature results @0.8 lpm

No Bimetal_ 1 lpm					Delta T
	Source 1	Source 2	Source 3	Source 4	
Case 1	37.9076	48.8953	46.5633	36.6796	12.2157
Case 2	28.0627	33.2581	42.5914	35.4406	14.5287
Case 3	36.619	44.8815	33.5045	28.1919	16.6896
Case 4	30.8338	43.9808	33.5324	34.6339	13.147
Case 5	35.3729	33.5655	42.0484	29.8945	12.1539

Table 12. No bimetal condition temperature results @ 1 lpm

No Bimetal_ 1.2 lpm					*Delta T*
	Source 1	*Source 2*	*Source 3*	*Source 4*	
Case 1	*37.0077*	*48.9699*	*46.0609*	*35.7482*	*13.2217*
Case 2	*27.8072*	*33.2112*	*42.1913*	*34.6807*	*14.3841*
Case 3	*35.88432*	*45.0003*	*33.4691*	*27.9393*	*17.061*
Case 4	*30.5171*	*44.1723*	*33.4819*	*33.966*	*13.6552*
Case 5	*34.6298*	*33.5317*	*41.7436*	*29.47*	*12.2736*

Table 13. No bimetal condition temperature results @ 1.2 lpm

No Bimetal_ 1.5 lpm					*Delta T*
	Source 1	*Source 2*	*Source 3*	*Source 4*	
Case 1	*36.1869*	*48.9676*	*44.2064*	*34.7938*	*14.1738*
Case 2	*27.547*	*32.601*	*40.7621*	*33.8803*	*13.2151*
Case 3	*35.1235*	*45.3042*	*32.9404*	*27.7243*	*17.5799*
Case 4	*30.2794*	*44.4907*	*32.9332*	*33.2755*	*14.2113*
Case 5	*33.8477*	*32.9221*	*40.3728*	*28.9513*	*11.4215*

Table 14. No bimetal condition temperature results @ 1.5 lpm

3.3.3 Simulation for with bimetal condition for all the cases

To perform the simulation with bimetal, condition the vent block are imported in the middle plate as shown in the figure 28. The opening to that particular block was taken from the deflection value of the bimetal from the table 15. Table 15. Was calculated in previous simulation of the bimetal and since the graph of the bimetal deflection vs temperature was liner, we can easily predict the value of the opening of the bimetal at specific temperature. To get the temperature reading at middle plate, temperature plot for upper face of the middle plate in each case of the no bimetal case was captured. And with that exact temperature value, respective bimetal deflection is provided to the blocks to control the flow.

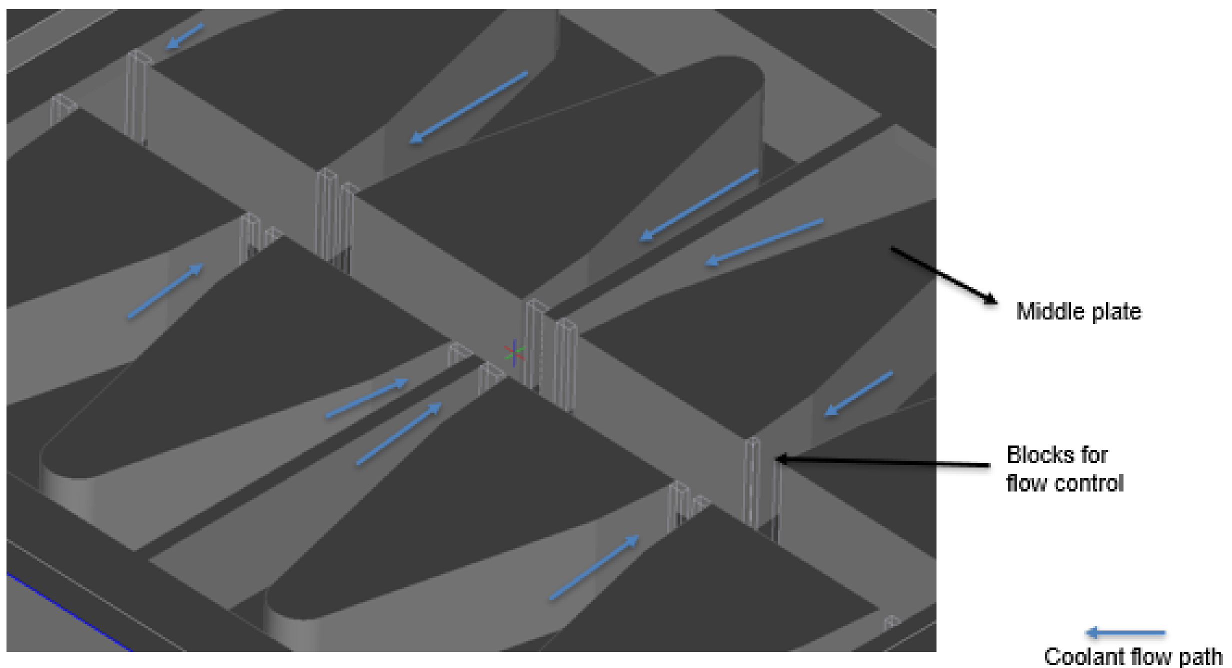

Figure 28. position of the blocks to replicate the opening created by bimetal

GB14- 50mm	
Y	X
Temp	Deflection, mm
25	0.13935
30	0.37159
35	0.60384
40	0.83608
45	1.0683
50	1.3006
55	1.5328
60	1.7651
65	1.9973
70	2.2296

Table 15. GB14 deflection at specific temperatures

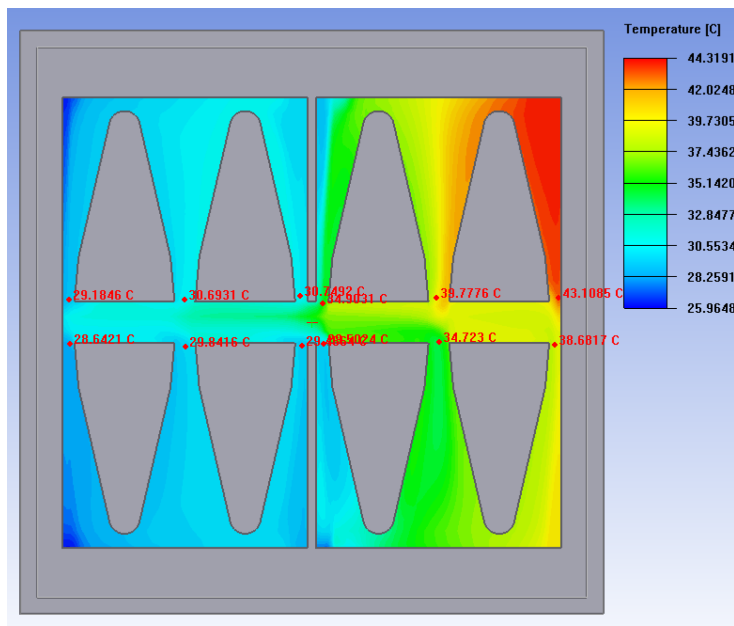

Figure 29. Top surface of middle plate CASE 1 @ 1 lpm

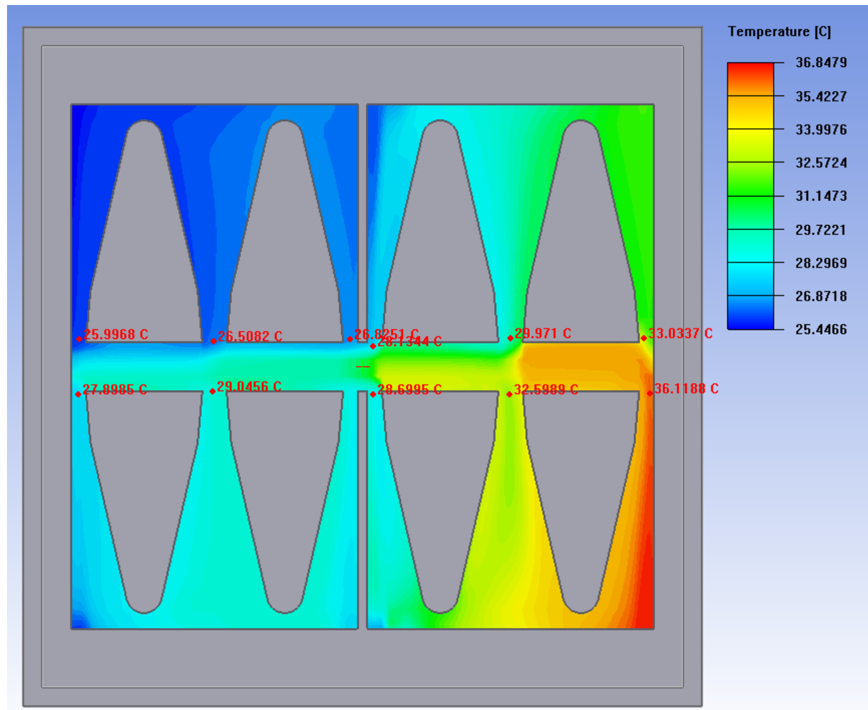

Figure 30. Top surface of middle plate CASE 2 @ 1 lpm

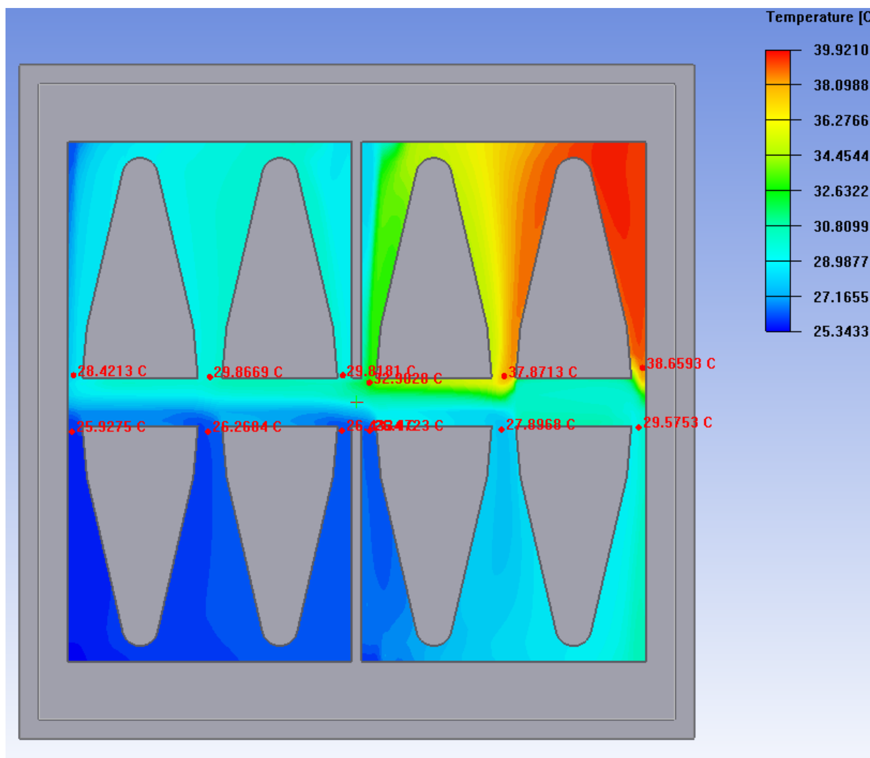

Figure 31. Top surface of middle plate CASE 3 @ 1 lpm

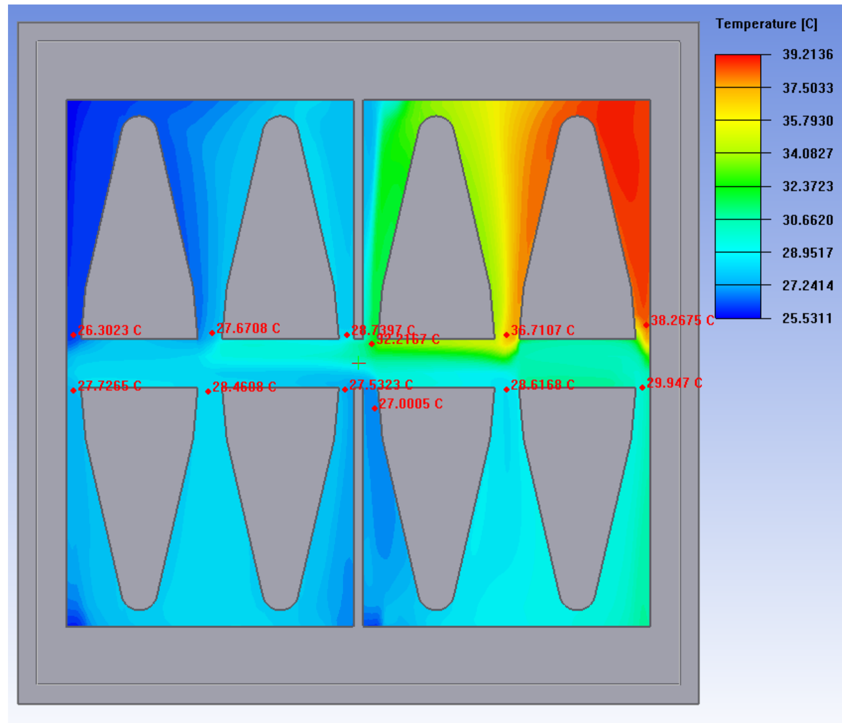

Figure 32. Top surface of middle plate CASE 4 @ 1 lpm

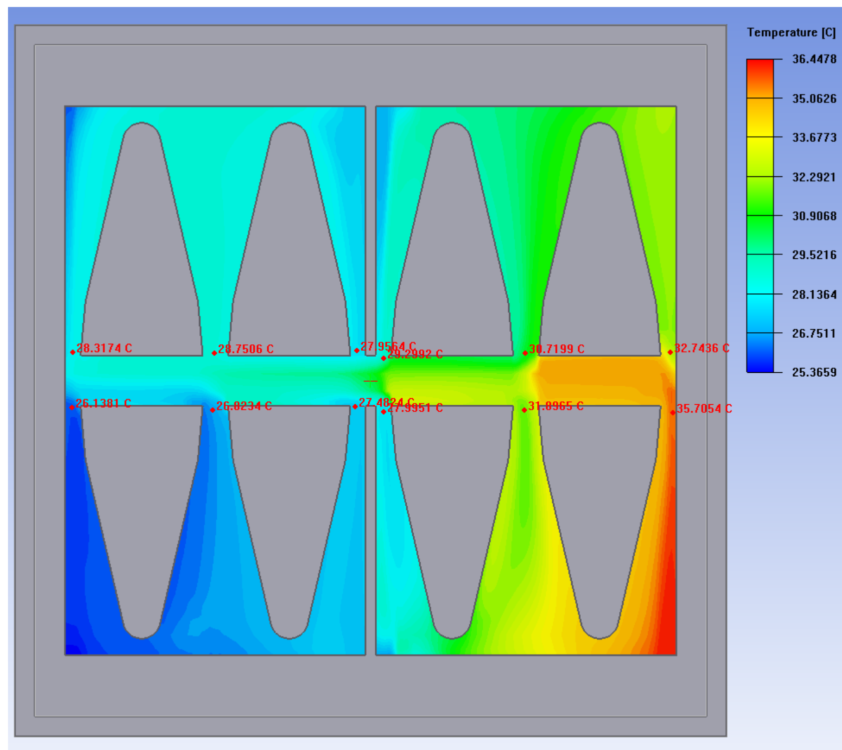

Figure 33. Top surface of middle plate CASE 5 @ 1 lpm

Figure 29-33 represents the top surface temperature for all the case at 1 lpm. Similarly, for all the lpm, temperatures were captured and the value of the temperature is used to get the deflection from the table 14.

3.3.4 Comparison between No-bimetal and with-bimetal cases

After importing block to the simulation to replicate the bimetal openings for each case for each lpm, result was plotted to see the temperature difference. Figure 34-38 represent the comparison of the temperature plot of the base of the cold plate for 0.6 lpm at each case between no bimetal and with bimetal simulation

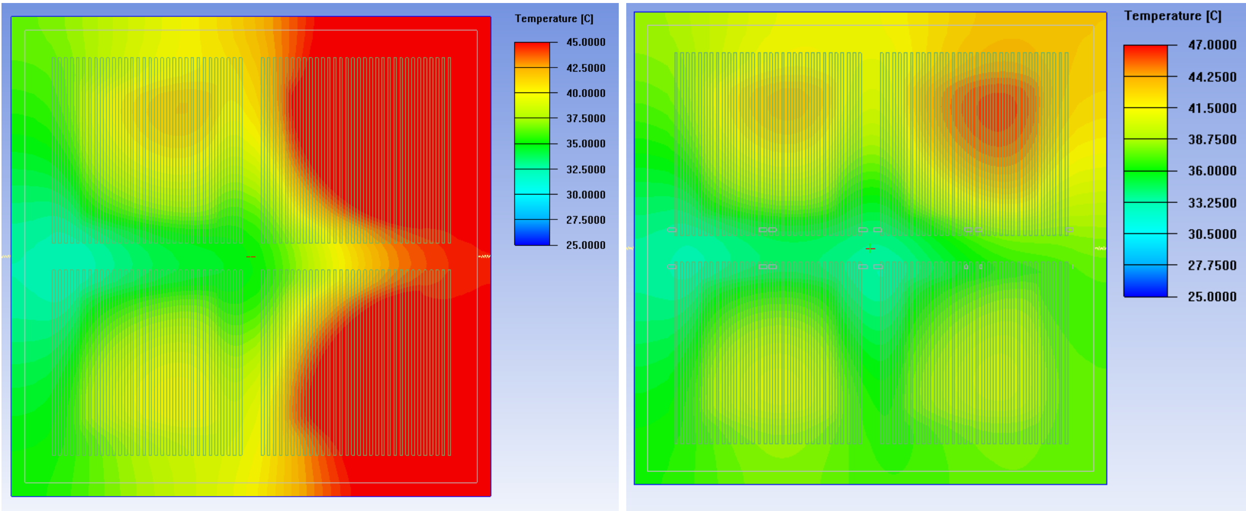

Figure 34. CASE 1 No bimetal (left), CASE 1 With bimetal (right)

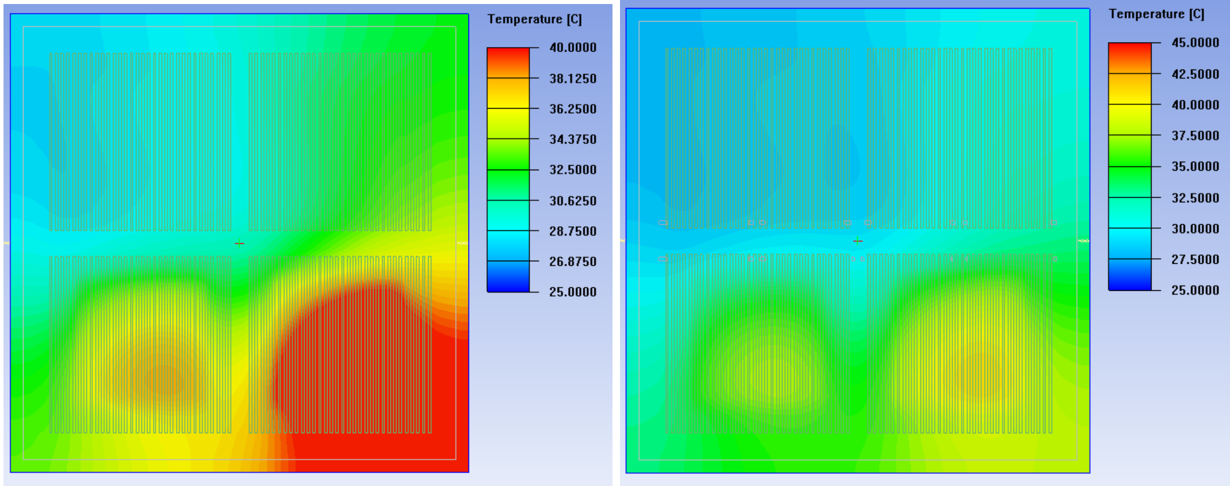

Figure 35. CASE 2 No bimetal (left), CASE 2 With bimetal (right)

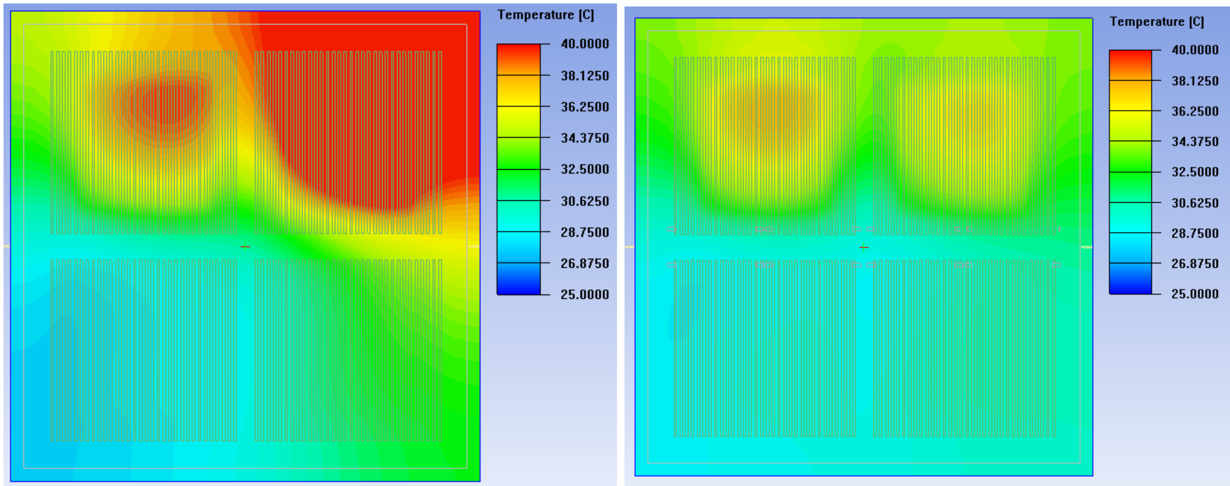

Figure 36. CASE 3 No bimetal (left), CASE 3 With bimetal (right)

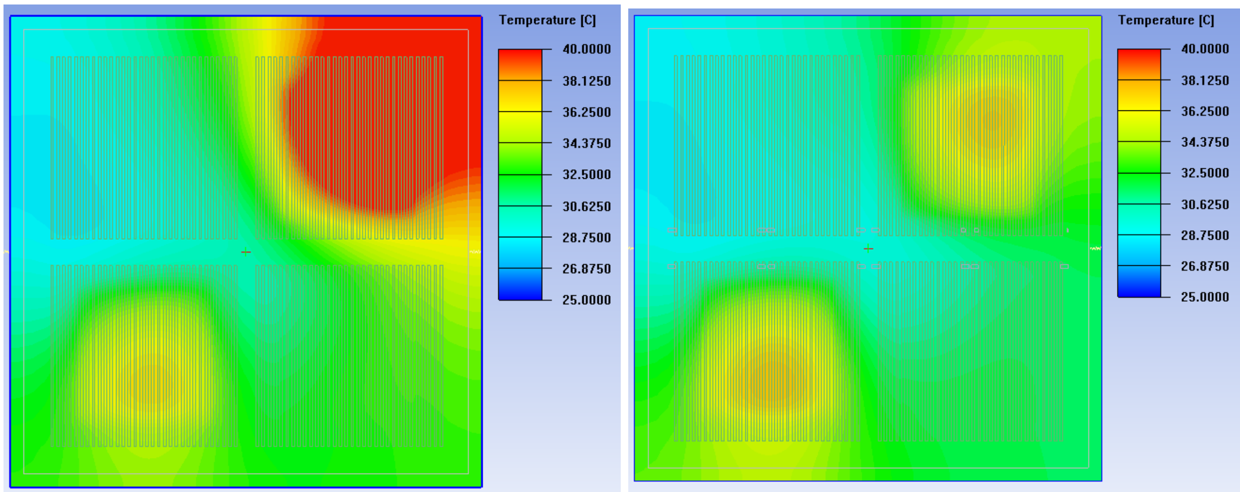

Figure 37. CASE 4 No bimetal (left), CASE 4 With bimetal (right)

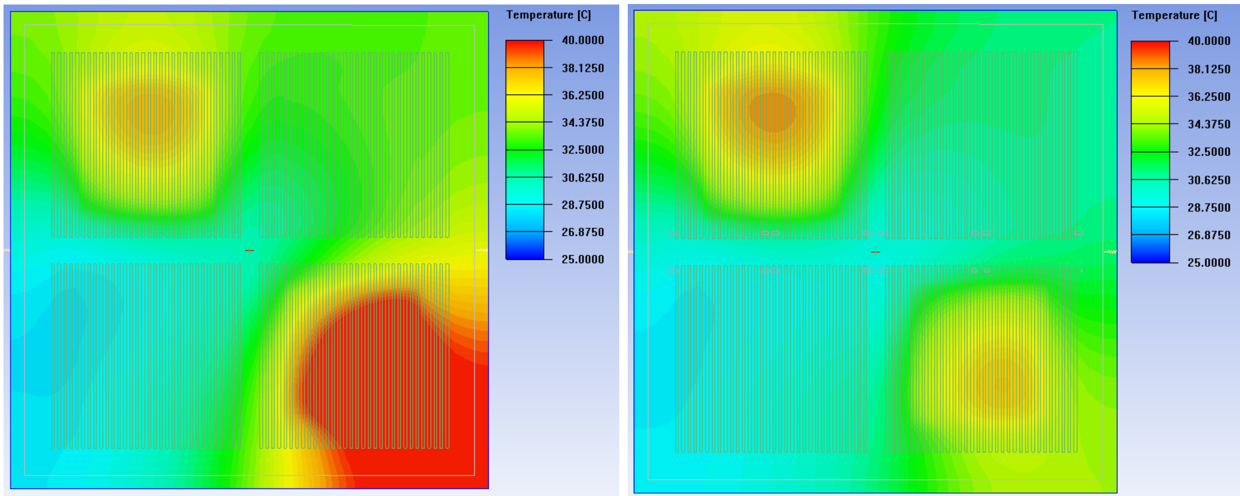

Figure 38. CASE 5 No bimetal (left), CASE 5 With bimetal (right)

Similar simulations are carried out for all the lpm and figure 39. Represents ΔT for all the cases at 0.6 lpm, 0.8 lpm, 1 lpm, 1.2 lpm, 1.5 lpm.

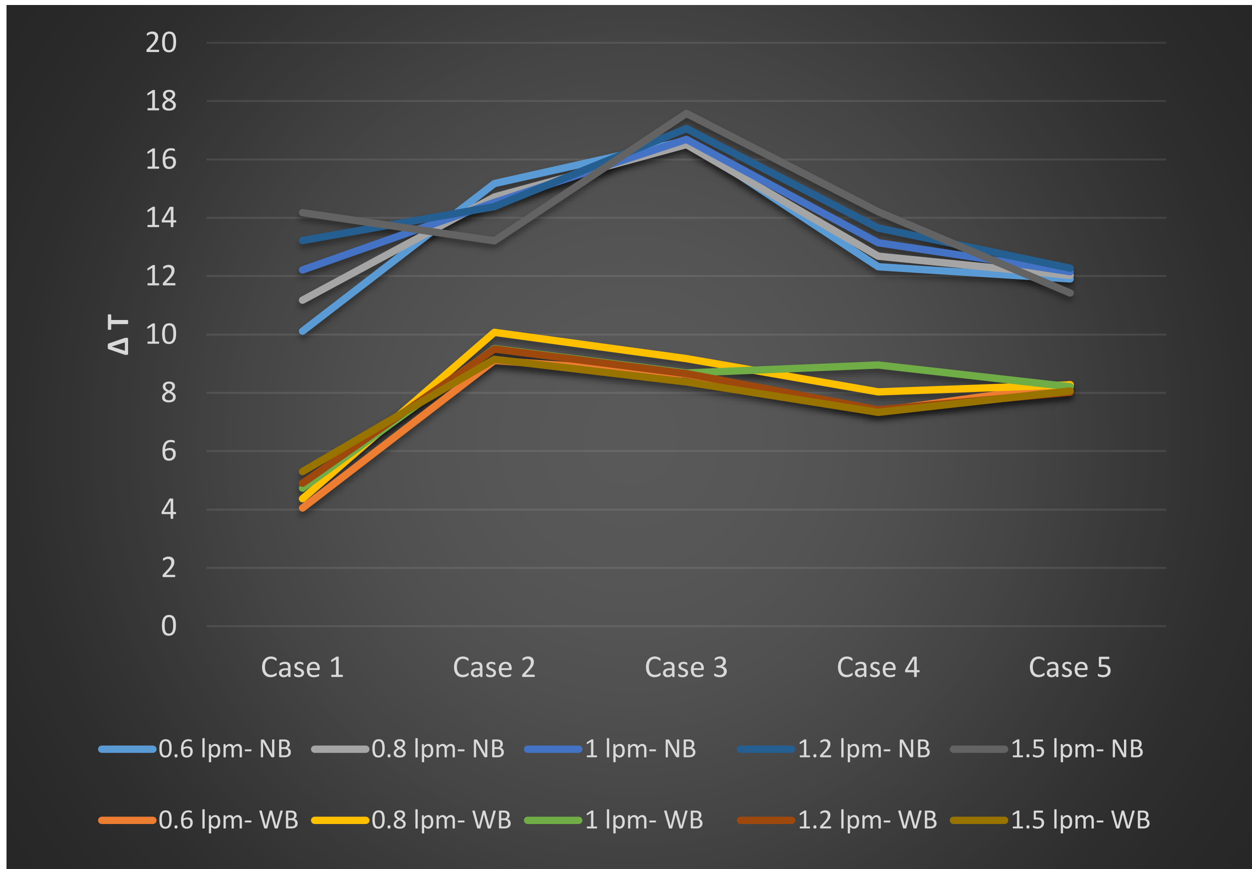

Figure 39. ΔT for all the cases at all lpm

Rth value for the cold plate plays vital role in performance assessment. It is calculated by following formula,

$$Rth = (T_{base} - T_{in})/Q \tag{4}$$

Tbase is the average of the temperature at the base of the cold plate, and it is taken from the both the simulation cases. Tin is the coolant inlet temperature and Q was the load heat load given to the cold plate.

Figure 40. represents the Rth for all the cases.

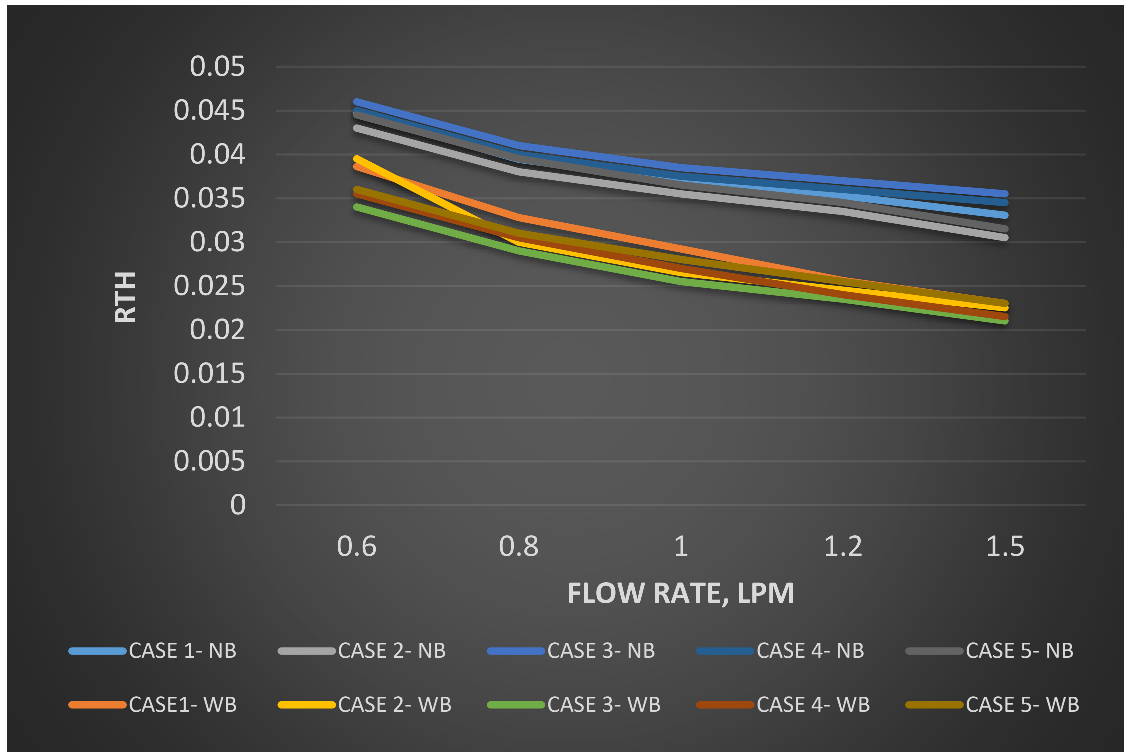

Figure 40. Rth for all the cases at all the lpm

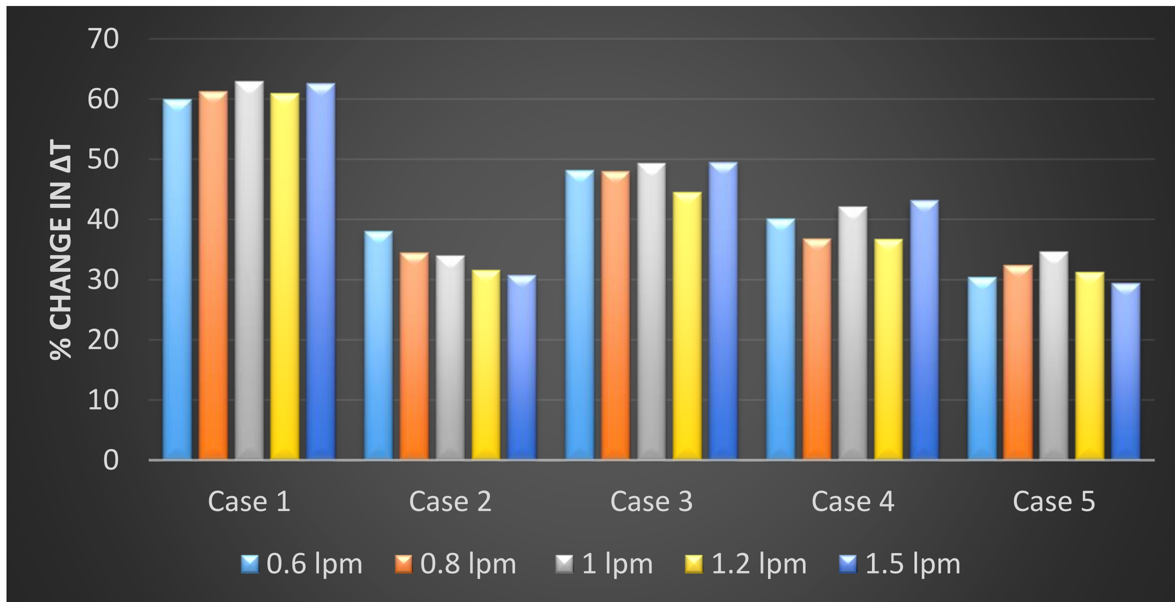

Figure 41. % Changes in temperature gradient for all the cases

Chapter 4

Conclusion and Future work

Dynamic cooling for direct to chip liquid cooling has researched in many previous studies and it has been proven as more efficient way of cooling than traditional air cooling [26-34]. In addition to single phase direct liquid cooling, implementation of the dynamic cooling control over each server and significantly improves the performance and can also surpass the performance of the 2 phase open bath immersion cooling by avoiding the issues like material compatibility and vapor pressure of 2- phase cooling system containing cold plates. [35-40]. Study on the retrofitted cold plates containing distributed pump flow suggested significant power saving [41]. A study on rack level dynamic cooling shown significant power saving when FCD made up of V-port ball valve was attached to the system to control the flow of the coolant thru each server [42]. FEA is a widely used analysis tool when any complicated simulation has to be evaluated. FEA can gives us accurate and correct results of different load condition, thermal condition, vibration analysis [43].

In this work the result of the both the simulation, No-bimetal, and With-bimetal cases, performed accurately as predicated. Flow control strategy thru bimetal was found to be effective as minimum 30% and maximum up to 62% of the reduction in the temperature gradient across the cold plate was observed. Rth defines the thermal performance of the system and suing dynamic cooling control thru fins can reduce the Rht value up to 40%. Traditional cold plate using conventional microchannel approach might not be sufficient for high hot spot modules and hence introducing dynamic cold plate could not only substantially improves the performance of the system but also improves the life of the component.

In the future work of this study dynamic simulation on 6SigmaET coupled with MATLAB can be performed to see the dynamic variation in the temperature on the top surface of cold plate. And

thru this, accurate flow variation can be seen. Experimental validation of this proposed idea is necessary and to do so, design of the cold plate must go under different design revision to get ready for manufacturability. Comparative study can be performed on experimental based result and more robust cold plate design can be achieved.

References

[1] Gao, T., Tang, H., Cui, Y., and Luo, Z., 2018, "A Test Study of Technology Cooling Loop in a Liquid Cooling System," *17th IEEE Intersociety Conference on Thermal and Thermomechanical Phenomena in Electronic Systems (ITherm)*, San Diego, CA, 2018, pp. 740-747, doi: 10.1109/ITHERM.2018.8419519.

[2] Iyengar, M., 2010, "Energy Consumption of Information Technology Data Centers,"

J. Electron. Cool., 16(4), epub.

[3] Andy Lawrence, April 2020, "Data center PUEs flat since 2013", Accessed January 7, 2020, Global Uptime Institute Survey, https://journal.uptimeinstitute.com/data-center-pues-flat-since-2013/

[4] Hoang, C.H., Khalili, S., Ramakrisnan, B., Rangarajan, S., Hadad, Y., Radmard, V., Sikka, K., Schiffres, S. and Sammakia, B., 2020, "An Experimental Apparatus for Two-phase Cooling of High Heat Flux Application using an Impinging Cold Plate and Dielectric Coolant," *36th Semiconductor Thermal Measurement, Modeling & Management Symposium (SEMI-THERM)*, San Jose, CA, USA, 2020, pp. 32-38, doi: 10.23919/SEMI-THERM50369.2020.9142831.

[5] Shahi, P., Agarwal, S., Saini, S., Niazmand, A., Bansode, P., & Agonafer, D., 2020, "CFD Analysis on Liquid Cooled Cold Plate Using Copper Nanoparticles," Proceedings of the ASME 2020 International Technical Conference and Exhibition on Packaging and Integration of Electronic and Photonic Microsystems. ASME 2020 International Technical Conference and Exhibition on Packaging and Integration of Electronic and Photonic Microsystems. Virtual, Online. October 27–29,2020.V001T08A007. ASME. https://doi.org/10.1115/IPACK2020-2592

[6] Niazmand, A., Chauhan, T., Saini, S., Shahi, P., Bansode, P.V., & Agonafer, D., 2020, "CFD Simulation of Two-Phase Immersion Cooling Using FC-72 Dielectric Fluid." Proceedings of the ASME 2020 International Technical Conference and Exhibition on Packaging and Integration of Electronic and Photonic Microsystems. ASME 2020 International Technical Conference and Exhibition on Packaging and Integration of Electronic and Photonic Microsystems. Virtual, Online. October 27–29, 2020. V001T07A009. ASME. https://doi.org/10.1115/IPACK2020-2595

[7] Chu, R. C., Simons, R. E., Ellsworth, M. J., Schmidt, R. R., and Cozzolino, V., 2004, "Review of Cooling Technologies for Computer Products," IEEE Trans. Device Mater. Reliab., 4(4), pp. 568–585.

[8] Ellsworth, M. J., Campbell, L. A., Simons, R. E., Iyengar, M. K., Schmidt, R. R., and Chu, R. C., 2008, "The Evolution of Water Cooling for Large IBM Large Server Systems: Back to the Future," 11th Intersociety Conference on Thermal and Thermomechanical Phenomena in Electronic Systems (ITherm), Orlando, FL, May 28–31, pp. 266–274.

[9] McFarlane, R., 2012, "Will Water-Cooled Servers Make Another Splash in the Data Center?," Tech Target Network, Search Data Center, Newton, MA, accessed Feb. 26, 2012,

https://searchdatacenter.techtarget.com/tip/Will-watercooled-servers-make-another-splash-in-the-data-center

[10] Schmidt, R. R., 2005, "Liquid Cooling Is Back," Electronics Cooling, 11(3), (epub).

[11] Patrizio, A., 2018, "Lenovo Introduces New Water-Cooled Server Technology," Network World, Framingham, MA, accessed Feb. 26, 2018, https://www.networkworld.com/article/3258646/data-center/lenovo-introduces-newwater-cooled-server-technology.html

[12] Koblentz, E., 2018, "How to Get Started With Liquid Cooling for Servers and Data Center Racks," Data Centers Trends Newsletter, TechRepublic, US edition, accessed July 8, 2018, https://www.techrepublic.com/article/how-to-getstarted-with-liquid-cooling-for-servers-and-data-center-racks/

[13] Iyengar, M., David, M., Parida, P., Kamath, V., Kochuparambil, B., Graybill, D., Schultz, M., Gaynes, M., Simons, R., Schmidt, R., and Chainer, T., 2012, "Server Liquid Cooling With Chiller-Less Data Center Design to Enable Significant Energy Savings," 28th Annual IEEE Semiconductor Thermal Measurement and Management Symposium (SEMI-THERM), San Jose, CA, Mar. 18–22, pp. 212–223.

[14] Fan, Y., Winkel, C., Kulkarni, D., and Tian, W., 2018, "Analytical Design Methodology for Liquid Based Cooling Solutions for High TDP CPUs," 17th IEEE Intersociety Conference on Thermal and Thermomechanical Phenomena in Electronic Systems (ITherm), San Diego, CA, May 29–June 1, pp. 582–586.

[15] Boucher, T. D., Auslander, D. M., Bash, C. E., Federspiel, C. C., and Patel, C. D. (November 11, 2005). "Viability of Dynamic Cooling Control in a Data Center Environment." ASME. *J. Electron. Packag*. June 2006; 128(2): 137–144. https://doi.org/10.1115/1.2165214

[16] Zhang, Y. et al. "Thermal Evaluation of 2.5-D Integration Using Bridge-Chip Technology: Challenges and Opportunities." IEEE Transactions on Components, Packaging and Manufacturing Technology 7 (2017): 1101-1110

[17] Gandhi, Dynamic Server Provisioning for Data Center Power Management, pp. 1-174, June 2013.

[18] K. Hazelwood, S. Bird, D. Brooks, S. Chintala, U. Diril, D. Dzhulgakov, et al., "Applied Machine Learning at Facebook: A Datacenter Infrastructure Perspective", *IEEE International Symposium on High Performance Computer Architecture (HPCA)*, Vienna, 2018, pp. 620-629, doi: 10.1109/HPCA.2018.00059.

[19] V. K. Arghode, V. Sundaralingam and Y. Joshi, 2016, "Airflow Management in a Contained Cold Aisle Using Active Fan Tiles for Energy Efficient Data- Center Operation Airflow Management in a Contained Cold Aisle Using Active Fan Tiles for Energy Efficient Data-Center, Heat Transfer Engineering, 37:3-4, 246-256, DOI: 10.1080/01457632.2015.1051386

[20] S. Khalili, G. Mohsenian, A. Desu, K. Ghose and B. Sammakia, "Airflow Management Using Active Air Dampers in Presence of a Dynamic Workload in Data Centers," *35th Semiconductor Thermal Measurement, Modeling and Management Symposium (SEMI-THERM), San Jose, CA, USA, 2019, pp. 101-110.*.

[21] H. Xu, C. Feng and B. Li, "Temperature Aware Workload Management in Geo-Distributed Data Centers," in *IEEE Transactions on Parallel and Distributed Systems*, vol. 26, no. 6, pp. 1743-1753, 1 June 2015, doi:10.1109/TPDS.2014.2325836.

[22] Kasukurthy, Rajesh, 2019, "Design and Optimization of Energy Conserving Solutions in Data Center Application," PhD dissertation, The University of Texas at Arlington, Arlington, TX.

[23] Kasukurthy, R., Rachakonda, A., and Agonafer, D., November 6, 2020, "Design and Optimization of Control Strategy to Reduce Pumping Power in Dynamic Liquid Cooling," ASME. J. Electron. Packag. doi: https://doi.org/10.1115/1.4049018

[24] Rushi, Ruben, 2018, "experimental and analytical study of a self-regulated flow control device developed for dynamic cold-plates to cool high-power density multi-chip modules," Master's Thesis, The University of Texas at Arlington, Arlington, TX.

[25] Ansys® FLUENT, Release 2019R3, ANSYS Fluent User's Guide, [book and chapter reference name/numbers], ANSYS, Inc.

[26] Shah, J.M., Anand, R., Saini, S., Cyriac, R., Agonafer, D., Singh, P., & Kaler, M., 2019, "Development of a Technique to Measure Deliquescent Relative Humidity of Particulate Contaminants and Determination of the Operating Relative Humidity of a Data Center, " Proceedings of the ASME 2019 International Technical Conference and Exhibition on Packaging and Integration of Electronic and Photonic Microsystems. ASME 2019 International Technical Conference and Exhibition on Packaging and Integration of Electronic and Photonic Microsystems. Anaheim, California, USA. October 7–9, 2019. V001T02A016. ASME. https://doi.org/10.1115/IPACK2019-6601

[27] Saini, Satyam, 2018, "Airflow Path and Flow Pattern Analysis of Sub-Micron Particulate Contaminants in a Data Center with Hot Aisle Containment System Utilizing Direct Air Cooling," The University of Texas at Arlington, Arlington, TX.

[28] Saini, S., Shahi, P., Bansode, P., Siddarth, A., Agonafer, D., 2020, "CFD Investigation of Dispersion of Airborne Particulate Contaminants in a Raised Floor Data Center," 36th Semiconductor Thermal Measurement, Modeling & Management Symposium (SEMI-THERM), San Jose, CA, USA, 2020, pp. 39-47, doi: 10.23919/SEMITHERM50369.2020.9142865.

[29] Thirunavakkarasu, G., Saini, S., Shah, J.M., Agonafer, D., 2018, "Air Flow Pattern and Path Flow Simulation of Airborne Particulate Contaminants in a High-Density Data Center Utilizing

Airside Economization," Proceedings of the ASME 2018 International Technical Conference and Exhibition on Packaging and Integration of Electronic and Photonic Microsystems. ASME 2018 International Technical Conference and Exhibition on Packaging and Integration of Electronic and Photonic Microsystems. San Francisco, California, USA. August 27–30, 2018. V001T02A011. ASME. https://doi.org/10.1115/IPACK2018-8436

[30] Saini, S., Adsul, K.K., Shahi, P., Niazmand, A., Bansode, P., & Agonafer, D., 2020, "CFD Modeling of the Distribution of Airborne Particulate Contaminants Inside Data Center Hardware," Proceedings of the ASME 2020 International Technical Conference and Exhibition on Packaging and Integration of Electronic and Photonic Microsystems. ASME 2020 International Technical Conference and Exhibition on Packaging and Integration of Electronic and Photonic Microsystems. Virtual, Online. October 27–29, 2020. V001T08A005. ASME. https://doi.org/10.1115/IPACK2020-2590

[31] Saini, S., Shah, J. M., Shahi, P., Bansode, P. V., Agonafer, D., Singh, P., Schmidt, R., and Kaler, M. (May 23, 2021). "Effects of Gaseous and Particulate Contaminants On Information Technology Equipment Reliability - A Review." ASME. *J. Electron. Packag*. doi: https://doi.org/10.1115/1.4051255

[32] Dehkordi BG, Fallah S, Niazmand A. Investigation of harmonic instability of laminar fluid flow past 2D rectangular cross sections with 0.5–4 aspect ratios. Proceedings of the Institution of Mechanical Engineers, Part C: Journal of Mechanical Engineering Science. 2014;228(5):828-839. doi:10.1177/0954406213491906

[33] Niazmand A, Fathi Sola J, Alinejad F, Rahimi Dehgolan F. Investigation of Mixed Convection in a Cylindrical Lid Driven Cavity Filled with Water-Cu Nanofluid. *Inventions*. 2019; 4(4):60. https://doi.org/10.3390/inventions4040060

[34] Shah, J. M., Anand, R., Singh, P., Saini, S., Cyriac, R., Agonafer, D., and Kaler, M. (June 23, 2020). "Development of a Precise and Cost-Effective Technique to Measure Deliquescent Relative Humidity of Particulate Contaminants and Determination of the Operating Relative Humidity of a Data Center Utilizing Airside Economization." ASME. J. Electron. Packag. December 2020; 142(4): 041103. https://doi.org/10.1115/1.4047469

[35] Gandhi, D., Chowdhury, U., Chauhan, T., Bansode, P.V., Saini., S, Shah, J.M., & Agonafer, D., 2019, "Computational Analysis for Thermal Optimization of Server for Single Phase Immersion Cooling," Proceedings of the ASME 2019 International Technical Conference and Exhibition on Packaging and Integration of Electronic and Photonic Microsystems. ASME 2019 International Technical Conference and Exhibition on Packaging and Integration of Electronic and Photonic Microsystems. Anaheim, California, USA. October 7–9, 2019. V001T02A013. ASME. https://doi.org/10.1115/IPACK2019-6587

[36] Shinde, P.A., Bansode, P.V., Saini, S., Kasukurthy, R., Chauhan, T., Shah, J.M., & Agonafer, D., 2019, "Experimental Analysis for Optimization of Thermal Performance of a Server in Single Phase Immersion Cooling," Proceedings of the ASME 2019 International Technical Conference and Exhibition on Packaging and Integration of Electronic and Photonic

Microsystems. ASME 2019 International Technical Conference and Exhibition on Packaging and Integration of Electronic and Photonic Microsystems. Anaheim, California, USA. October 7–9, 2019. V001T02A014. ASME. https://doi.org/10.1115/IPACK2019-6590

[37] Bansode, P. V., Shah, J. M., Gupta, G., Agonafer, D., Patel, H., Roe, D., and Tufty, R. (November 8, 2019). "Measurement of the Thermal Performance of a Custom-Build Single-Phase Immersion Cooled Server at Various High and Low Temperatures for Prolonged Time." ASME. *J. Electron. Packag*. March 2020; 142(1): 011010. https://doi.org/10.1115/1.4045156

[38] Niazmand, A., Murthy, P., Saini, S., Shahi, P., Bansode, P., & Agonafer, D., 2020, "Numerical Analysis of Oil Immersion Cooling of a Server Using Mineral Oil and Al2O3 Nanofluid," Proceedings of the ASME 2020 International Technical Conference and Exhibition on Packaging and Integration of Electronic and Photonic Microsystems. ASME 2020 International Technical Conference and Exhibition on Packaging and Integration of Electronic and Photonic Microsystems. Virtual, Online. October 27–29, 2020. V001T08A009. ASME. https://doi.org/10.1115/IPACK2020-2662

[39] Kumar, A., Shahi, P., Saha, S.K., 2018, "Experimental study of latent heat thermal energy storage system for medium temperature solar applications," In Proceedings of the 4th World Congress on Mechanical, Chemical, and Material Engineering (MCM'18), Madrid, Spain, pp. 16-18.

[40] Hoang, C.H., Khalili, S., Ramakrisnan, B., Rangarajan, S., Hadad, Y., Radmard, V., Sikka, K., Schiffres, S. and Sammakia, B., 2020, March, "An Experimental Apparatus for Two-phase Cooling of High Heat Flux Application using an Impinging Cold Plate and Dielectric Coolant," In *2020 36th Semiconductor Thermal Measurement, Modeling & Management Symposium (SEMI-THERM)*, pp. 32-38, doi: 10.23919/SEMI-THERM50369.2020.9142831.

[41] Shahi, P., Saini, S., Bansode, P., and Agonafer, D., 2021, "A Comparative Study of Energy Savings in a Liquid-Cooled Server by Dynamic Control of Coolant Flow Rate at Server Level," in IEEE Transactions on Components, Packaging and Manufacturing Technology, 11(4), pp. 616-624, doi: 10.1109/TCPMT.2021.3067045.

[42] Shahi, P., Deshmukh, A.P., Hurnekar, H.Y., Saini, S., Bansode, P., Kasukurthy, R., Agonafer, D., 2021, "Design, Development and Characterization of a Flow Control Device for Dynamic Cooling Liquid Cooled Servers," ASME Journal of Electronic Packaging.

[43] A. Lakshminarayana, A. Misrak, R. Bhandari, T. Chauhan, A. S. M. R. Chowdhury, and D. Agonafer, "Impact of Viscoelastic Properties of Low Loss Printed Circuit Boards (PCBs) on Reliability of WCSP Packages Under Drop Test," in *2020 IEEE 70th Electronic Components and Technology Conference (ECTC)*, 2020, pp. 2266–2271, doi:10.1109/ECTC32862.2020.00353.